12-10-2010

Identification Of Measurement Technology For Online Recording Of Transients In Underground Residential Distribution System

Balaji Pushpanathan

IDENTIFICATION OF MEASUREMENT TECHNOLOGY FOR ONLINE RECORDING OF TRANSIENTS IN UNDERGROUND RESIDENTIAL DISTRIBUTION SYSTEM

By

Balaji Pushpanathan

A Thesis
Submitted to the Faculty of
Mississippi State University
in Partial Fulfillment of the Requirements
for the Degree of Master of Science
in Electrical Engineering
in the Department of Electrical and Computer Engineering

Mississippi State, Mississippi

December 2010

IDENTIFICATION OF MEASUREMENT TECHNOLOGY FOR ONLINE RECORDING OF TRANSIENTS IN UNDERGROUND RESIDENTIAL DISTRIBUTION SYSTEM

By

Balaji Pushpanathan

Approved:

Stanislaw Grzybowski Professor of Electrical and Computer Engineering (Major Advisor and Director of Thesis)	Nicolas H. Younan Department Head and Professor of Electrical and Computer Engineering (Committee Member)
Clayborne D. Taylor, Jr. Assistant Research Professor of Electrical and Computer Engineering (Committee Member)	James E. Fowler Professor of Electrical and Computer Engineering (Graduate Coordinator)

Lori Bruce
Associate Dean of College of Engineering

Name: Balaji Pushpanathan

Date of Degree: December 10, 2010

Institution: Mississippi State University

Major Field: Electrical Engineering

Major Professor: Stanislaw Grzybowski

Title of Study: IDENTIFICATION OF MEASUREMENT TECHNOLOGY FOR ONLINE RECORDING OF TRANSIENTS IN UNDERGROUND RESIDENTIAL DISTRIBUTION SYSTEM

Pages in Study: 80

Candidate for Degree of Master of Science

Underground Residential Distribution (URD) power cables are aged due to electrical, thermal, mechanical, and environmental stresses during their service. The recent dielectric conditions of the cables are of much interest for utilities. The existing offline diagnostic method requires forceful disconnection of the URD cable for maintenance. Online recording and Fast Fourier Transform analysis of intentionally created transients in URD is one of the promising methods to assess the current condition of the cable. For the larger goal of developing an online power cable condition assessment, the measurement techniques, which are required to be implemented, have to be evaluated. In order to implement the online measurement system, the requirements of the measurement system have to first be identified. URD system model was simulated using the Electro Magnetic Transient Program to identify the characteristics of induced transients. A list of requirements of the measurement system was created based on the simulation results.

DEDICATION

I would like to dedicate this research work to my parents, Mr. R. Pushpanathan, and Mrs. P. Thara, my undergraduate thesis advisor, Dr. S. Venkatesh, and my graduate major advisor, Dr. Stanislaw Grzybowski.

ACKNOWLEDGEMENTS

I express my sincere gratitude to all the people who provided their selfless assistance, without which this thesis could not have been materialized. First of all, I would like to thank Dr. Stanislaw Grzybowski, academic advisor, for his guidance and support throughout my graduate studies and research. I would like to thank all the staff at the San Diego Gas & Electric's Skills Training facility, in particular, Dr. Thomas Owen Bialek, Mr. Ronald Jordan, and Mr. William Torre for providing me with the needed support. I would like to thank Dr. Nicolas Younan and Dr. Clayborne Taylor, Jr. for their valuable advice through the course of my studies and review of my work. My sincere thanks to technical staff and graduate students of the Mississippi State University High Voltage Laboratory for their assistance and cooperation provided throughout my research.

TABLE OF CONTENTS

Page

LIST OF TABLES

LIST OF FIGURES

CHAPTER I

INTRODUCTION

1.1 Importance of Online Diagnostic Methods of the URD System

Underground Residential Distribution (URD) power cables are aged due to electrical, thermal, mechanical and environmental stresses during their service. The recent dielectric conditions of the cables are of much interest for utilities. Some destructive and non-destructive methods are available to estimate the actual status of the cable insulation [20, 21]. These tests are based on AC sources of different frequency ranges, DC sources and impulse sources [26, 27]. The DC tests on cables are reported to stress the cable to unusual voltage stress because the DC potential causes many cables to fail during tests which will not fail under operating condition [31, 32, 33]. The VLF test does not simulate the stresses present in field conditions in the testing cable [35, 36]. To obtain a conclusive decision about the state of the cable insulation, a multitude of tests, specifically on-line, have to be performed [26]. One of the methods estimates the cable insulation condition by using Fast Fourier Transform (FFT) analysis of impulse wave propagation in URD cable systems [1, 9]. Offline methods such as transfer function, dielectric spectroscopy, and partial discharge methods are available to evaluate the condition of the cable [1, 6, 23, 7, 25, 34]. In frequency domain, division of voltage spectrum by current spectrum gives the transfer function [37]. It has been seen by various researchers that the movements in peak in frequency domain of the transfer function

indicate location of fault, and changes in amplitude indicate the partial discharge activities [37, 38, 39, 1].

Mobile on-site cable diagnostic devices have been used to diagnose cables based on harmonic loss currents [10, 30]. There are many tests performed by various organizations on combined waveform testing of cables to access the degradation [17, 18, 19, 22]. There are few online cable monitoring systems developed by superimposing DC voltage and by measuring the DC currents through ground connection for ungrounded, cross-linked polyethylene, XLPE cable systems [15, 16, 28].There are also few online testing apparatus designed for measuring the dielectric dissipation factor as a guidance of state of insulation [29]. The existing offline diagnostic method requires forceful maintenance removal of the cable from the URD to conduct diagnostic tests. Continuous online recording of transients in URD will help to monitor the current condition of electrical insulation. The assessment of the cables in URD helps utilities prioritize their scheduled maintenance work on the cable.

1.2 Motivation

Smart grid vision requires prioritizing the scheduling of the maintenance on Underground Residential Distribution (URD) based on the condition of the cables of the URD. In order to achieve this vision, the condition of the cables of URD has to be continuously assessed while they are in service. The cable insulation parameters of the cables have to be extracted without removing the cables from the service. Intentionally inducing an acceptable transient in URD and recording the transients appearing at the various locations of the URD will extract the insulation parameters of the cables in the URD. So as to induce and record acceptable transients in the URD, a transient source and

measurement system for live (online) connections and measurements is identified in this work.

1.3 Outline of the Study

For implementation of continuous online recording of transients in URD, proper measurement technology needs to be identified in order to induce transients and to capture the transients along the length of the URD. Simulation was chosen as a tool to identify the characteristics of transients propagating in URD. By characterizing the transients using simulations, the necessary measuring equipments were identified and proper test plans were devised.

In this study, a typical radial URD system was modeled by using EMTP for transient studies. Simulation of the non-energized system model was compared with transients recorded on an open-ended cable thumped at SDG&E. Based on the verification of the non-energized cable model, an energized URD was modeled in EMTP. Thumpers or pulse generators were modeled and simulated to induce transients in the model URD. The model was simulated for different thumper pulse voltage, energy, and operating conditions of the URD to identify the effect of various operating conditions on the nature of the transients.

Results of the simulations were used to identify the peak voltage, peak current, and the duration of the transients. Discrete Fourier analysis (DFT) was performed on the simulation results using MATLAB. Using the DFT, the frequency spectrum and the bandwidth requirements were identified. Digital quantization noise, which will appear due to signal processing of data, was simulated using MATLAB to identify the required vertical resolution.

The simplified co-axial cable model representing the simulated cable was analyzed using MATLAB for travelling waves and related attenuation issues. Literature review helped to identify the effects of various types of noise and different ways to mitigate noise issues for differential measurement. Based on the analysis of the simulations, measurement system's connection methodology and test plan was devised for a pilot project for utilities.

CHAPTER II

SIMULATION

2.1 Simplified Cable Model

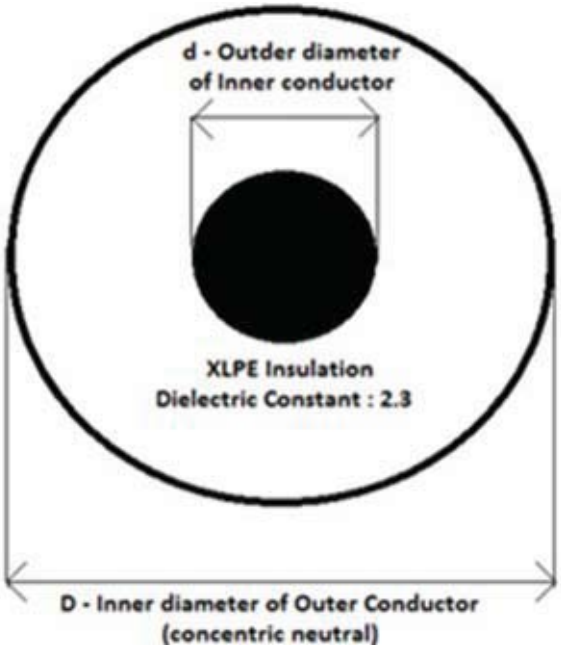

Figure 2.1 Cable Configuration

A simplified cable of dimensions similar to the 1000 kcmil XLPE 600A cable is shown in Fig. 2.1. The effect of the internal stranded conductor is to reduce the skin effect at power frequency. The basic co-axial cable model was used for discussion of attenuation in the cable, and for conservative analysis, while the internal conductor in the basic model was considered a solid conductor.

2.1.1 Cable Parameters

The Specifications of the cable shown in Figure 2.1 are follows [2]:

Inner radius (d/2) = 14.1859 mm

Outer radius (D/2) = 21.0439 mm

Aluminium conductor conductivity = 3.55 * 10^7 S/m

Aluminium conductor relative permeability μ = 1

Insulation relative permittivity εr = 2.3

For the cable shown in Fig. 2.1, the Traverse Electro Magnetic (TEM) parameters were calculated as follows:

Inductance calculation [4]:

$L = 2 * 10^{-7} * \ln\left(D/d\right)$ H/m Eq. 2.1

L = 78.87 nH/m

Capacitance calculation [4]:

$C = (2 * \pi * \varepsilon r * \varepsilon_0)/\ln\left(D/d\right)$ H/m Eq. 2.2

C = 0.3245 nF/m

Velocity calculation [4]:

$V = 1/\sqrt{(L * C)}$ m/s Eq. 2.3

v = 198 * 10 m/s

v = 198 m/μs

v = 650 feet/μs

Characteristic impedance [4]:

$Z = \sqrt{L/C}$ Eq. 2.4

Z = 16

2.1.2 Travelling wave model

Any applied voltage on a conductor can be seen as a wave travelling on the conductors. Speed of the voltage and current travelling in conducting medium is governed by the material and geometric properties of the conducting medium and its surrounding medium. As the wave travels along the conductor, it gets attenuated depending upon the material property. In addition to attenuation, the waves get partially reflected at every discontinuity of impedance. Complete reflection occurs at termination (open or short). After a significant number of reflections and attenuation, on maintaining steady state voltage application, standing wave voltage profiles are formed for AC, and a constant voltage profile (DC) is formed across the conductor length [3].

It was also observed that wave propagation parameters are different for different frequencies of waves imposed.

A simple co-axial cable was considered for analysis of the travelling waves. The applied voltage of interest has characteristics of impulse voltage. The frequency domain of the applied impulse was resolved into different frequency components. Every frequency component can be represented as cosine waveform. Hence, attenuation along the length of the cable for each component can be computed by TEM mode analysis of the coaxial cable [4].

$$v(z,t) = Vo^{+} * \cos(\omega t - \beta z + \emptyset^{+}) * e^{-\alpha z} + Vo6 * \cos(\omega t + \beta z + \emptyset 6) * e^{\alpha z} \quad \text{Eq. 2.5}$$

Where

v, voltage at any point in the length of conductor at any time in voltage,

Vo^{+}, initial amplitude of voltage wave travelling at positive direction,

$Vo6$, initial amplitude of voltage wave travelling at negative direction,

t, time in second,

z, distance from reference,

ω, frequency in radian/second,

β, phase constant,

$\emptyset$, reference phase,

α, attenuation constant

In the TEM equation 2.5, (αz), the attenuation determines the level of signal attenuation along the length of the cable. Hence the attenuation factor plays a vital role in determining the strength of the signal along the cable.

Attenuation factor was calculated as per Eq 2.6, as follows:

$$\alpha = Real(\sqrt{(R + j\omega L)(G + j\omega C)}) \qquad \text{Eq. 2.6}$$

Where,

$$R = \sqrt{\frac{f}{4*\sigma*\pi}} * \left(\frac{2}{D} + \frac{2}{d}\right) \quad \text{in } \Omega/m \qquad \text{Eq. 2.7}$$

$$G = \sqrt{\frac{4*\pi^2*f*\varepsilon*tan\delta}{log\frac{D}{d}}} \quad \text{in S/m} \qquad \text{Eq. 2.8}$$

$$C = 2 * \pi * \varepsilon * \varepsilon_0 * \frac{1}{\log\left(\frac{D}{d}\right)} \quad \text{in F/m} \qquad \text{Eq. 2.9}$$

$$L = 2 * 10^{-7} * ln\left(\frac{D}{d}\right) \quad \text{in H/m} \qquad \text{Eq. 2.10}$$

2.2 EMTP

The transients in the model Underground Residential Distribution (URD) can be analyzed using equations, simulations, and test setups. As first step, the test system was modeled in an Electro Magnetic Transient Program (EMTP) [14].

The transients can be analyzed by using equations governing time domain wave propagation. In this type of simulation, the medium is modeled for time domain differential equations, mostly with fixed lumped parameters. The propagating wave can be solved from the complex equations of the time domain model. This type of analysis is straightforward, but is complex and very time consuming for systems of moderate complexity, which has much bifurcation in cables, as in the case of the radial feeder of SDG&E URD.

The transients can also be analyzed by frequency domain simulations, based on frequency dependent model parameters, which are very good, though transferring results to time domain creates problem for fast transients.

The simulations can also be analyzed by forming a frequency-dependent modal transformation matrix and running time domain simulations using the matrix. By this method, all the components are modeled based on frequency dependent components, and at the same time direct time domain simulations are performed on every time step.

The EMTP-RV software package was chosen based on its capability to solve 5000 devices using the frequency-dependent modal transformation matrix driven time domain simulation for step size in the order of nanoseconds.

2.2.1 EMTP-RV model

Two cables are modeled and prepared in the Electro Magnetic Transient Program (EMTP-RV). A 152.4 meter 1000 kcmil XLPE cable is modeled for primary feeder. A 91.44 meter 2/0 XLPE cable was modeled for branching feeder. Both cables are modeled based on the values provided by SDG&E data warehouse spreadsheet. The parameters of the cable are specified in Table 2.1.

Different URD models were created and simulated during the progress of the project. The final URD model of 2895.6 meter long radial primary feeder with 9 distribution feeder taps is simulated as shown in Fig. 2.2.

Table 2.1 Cable Dimensions

Cable name	1000 kcmil XLPE	2/0 XLPE
Conductor radius	14.2 mm	5.15 mm
Conductor type	Aluminium	Aluminium
Insulation thickness	6.9 mm	7.4 mm
Dielectric constant	2.3	2.3
Insulation loss factor	0.001	0.001
Jacket type	PE	PE
Outer radius	25.5 mm	14 mm
Ampere capacity	600 A	200 A

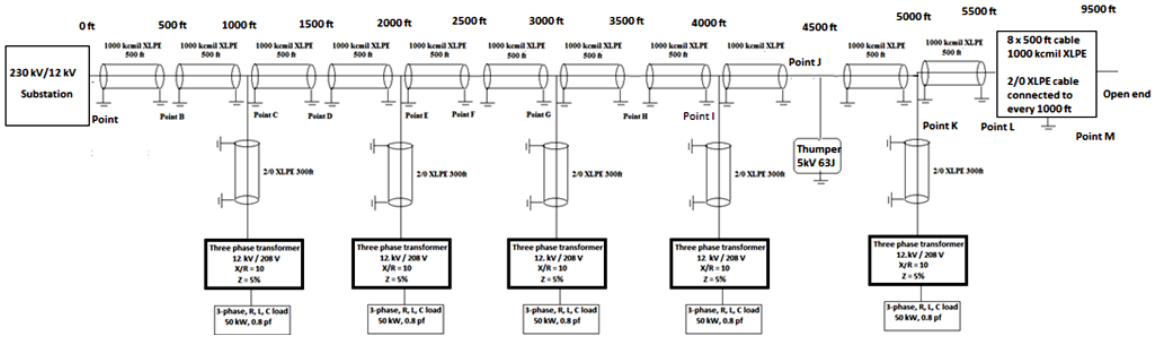

Figure 2.2 12 kV URD system model for simulation analysis

CHAPTER III

RESULTS AND ANALYSIS

In order to identify the parameters of the transients which will appear in the URD system, the URD system was modeled and simulated in EMTP-RV. Fast Fourier Transform (FFT) was used to convert the simulation results to frequency spectrum. MATLAB was used to run FFT programs. With the help of the simulation results, the requirements of measuring instruments were outlined. The progress towards achieving simulation model of energized cable system is presented in following sections.

3.1 Cable Model Simulation and Validation

To construct a valid cable model, the frequency content of the data sample provided by SDG&E was obtained using Fourier transformation, as shown in Fig. 3.1. The data provided by SDG&E consisted of a thumper test conducted on 30 m long XLPE insulated, aluminium conductor cable as shown in Fig. 3.1 [1]. Based on the cable warehouse data provided by SDG&E, a similar 30 m long XLPE open-ended cable was modeled in EMTP-RV. The result of the model simulation is shown in Fig. 3.2.

From Fig. 3.2 and Fig. 3.3, it is seen that the transient signals were around 2 MHz range. Two cables, (1000 kcmil XLPE and 2/0 XLPE), which are present in the test radial feeder distribution system provided by SDG&E, were modeled, and a sample URD system of 762 meter was simulated in EMTP-RV. Additional results of captured time domain and frequency domain results are presented in Appendix A.

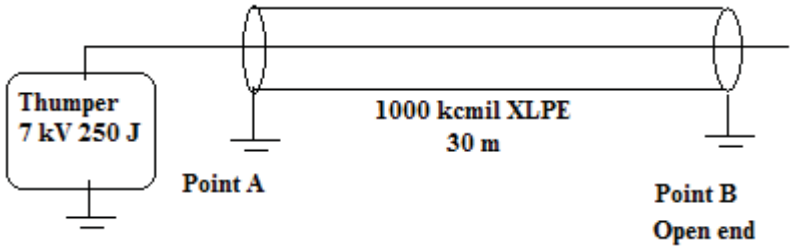

Figure 3.1 Open-ended 30 m cable model

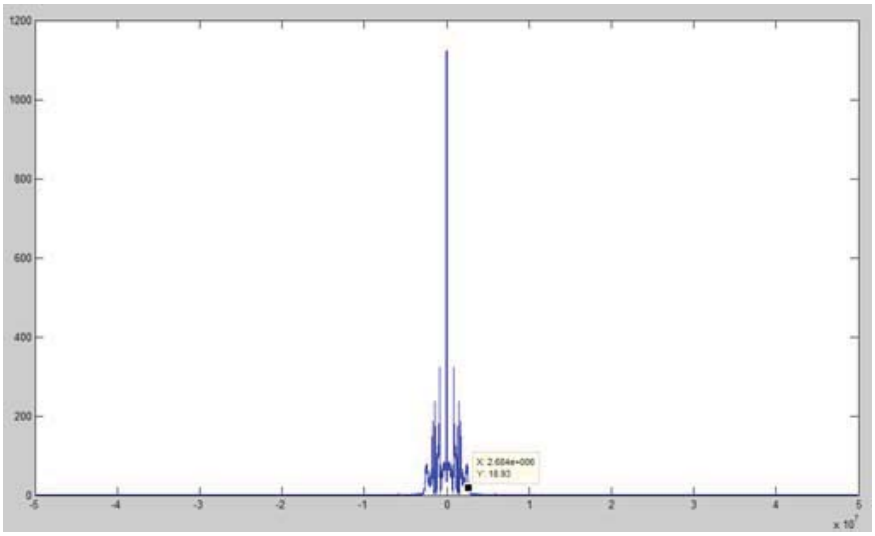

Figure 3.2 Freqency spectral data of Voltage (Data provided by SDG&E)

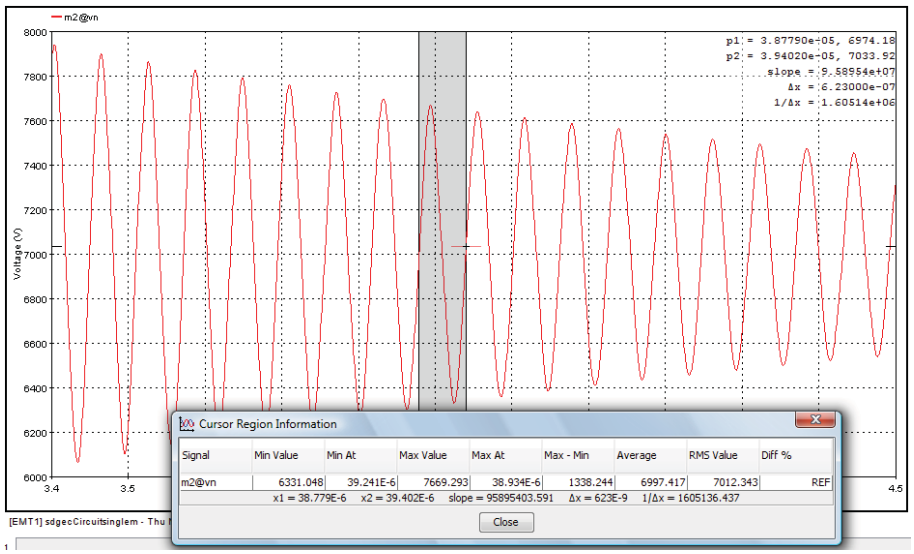

Figure 3.3 Voltage function time of voltage at thumper end (simulation)

3.2 Non-Energized URD system model simulation and analysis

Before proceeding to an energized URD system, a non-energized URD system of 762 and 2590.8 meter was modeled and simulated, and the results were analyzed for better understanding of the transients.

When a charged thumper is connected to the energized distribution cable, the applied voltage charges the cable, and the applied voltage impulse travels along the length of the cable with a velocity that depends on the L & C values of the cable. These impulses get reflected, refracted and split when they reach splices. The effect of the reflections is seen as oscillation of voltage and current at a single place with respect to time. In order to extract the impedance value of the cable from the recorded transients, the entire oscillations have to be measured with greater accuracy. The non-energized URD cable system model was simulated for 7 kV, 250 J, and Thumper's discharge at the starting of the radial feeder. The simulation was carried out using EMTP-RV. The results were analyzed using matlab. The model consists of 1000 kcmil XLPE 152.4 meter long cables as main feeder and 2/0 XLPE 91.44 meter cables as radial feeder feeding inductive

R-L load through 3-phase transformers. The non-energized URD cable system gives a starting reference to build a reliable model and a reference frequency spectrum of oscillations. Frequency spectrums (Discrete Fourier Transform, DFT) of the voltage at various points are observed for 762 meter long and 2590.8 meter long URD cables system. Fig. 3.4 shows the schematic of the simulated URD system.

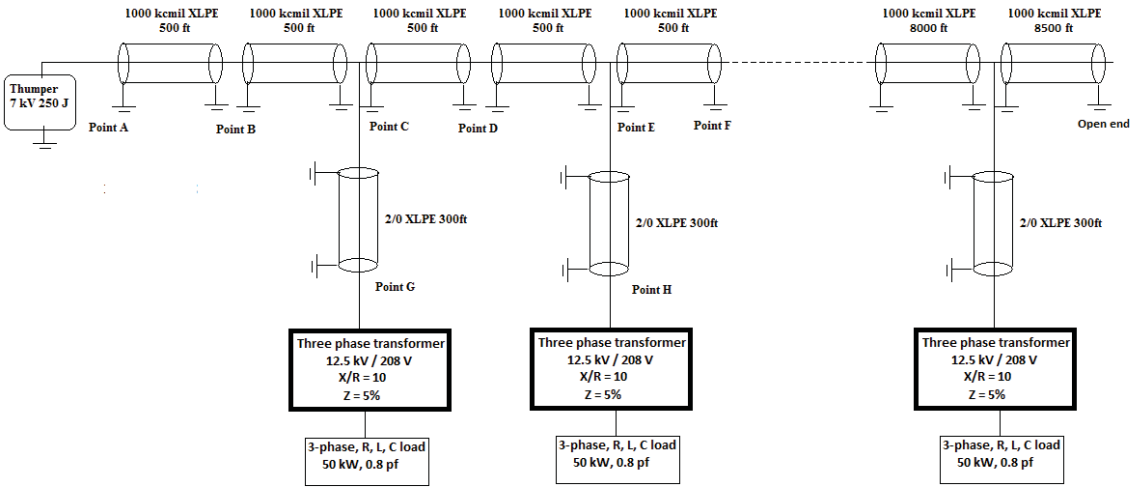

Figure 3.4 Test URD system up to 2590.8 meter (8500 feet)

For 762 meter long URD cable system simulation, peak voltage value occurs at the open end, Point F. It is nearly 15 kV, which is twice the applied thumper voltage. The initial impulse voltage arrives at 3.54 μs to 762 meter away from thumper, point F. This counts for the wave velocity of 215 m/μs. From the calculations presented in section 2.1.2, the wave velocity is 200 m/μs. The initial impulse voltage reaching various locations keeps attenuating from 7 kV at thumper end to 0.45 kV at 762 meter from thumper end.

Discrete Fourier Transform (DFT) of the signal was obtained using Fast Fourier Transform (FFT) using MATLAB. From the single-sided frequency response of the

voltage and current at all the waveforms, (example Fig. 3.6 and Fig. 3.7), magnitude of the voltage and current frequency components reduces to less than 1V and 1A, respectively, beyond 2 MHz.

More number of frequency components can be seen for longer cable length due to more reflection points, but the oscillations amplitude reduces after 2 MHZ. The pulse reflections from the transformer end create more high frequency oscillations due to multiple reflections from load terminations. But the oscillations does not completely changes the wave shape in the incoming and the outgoing cables, as the amplitude of the wave oscillation is less. The frequency spectrum of the current at the cable connecting to transformer has very low value as seen in Fig. 3.7. This suggests that the transformer de-couples fast transients and appears as a high impedance reflection point. Additional results of captured time domain and frequency domain results are presented in Appendix B.

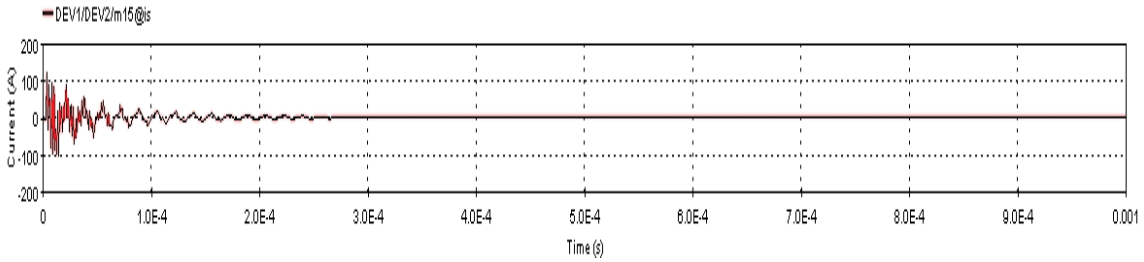

Figure 3.5 Current function time at 609.6 m from Thumper on radial cable, Point E

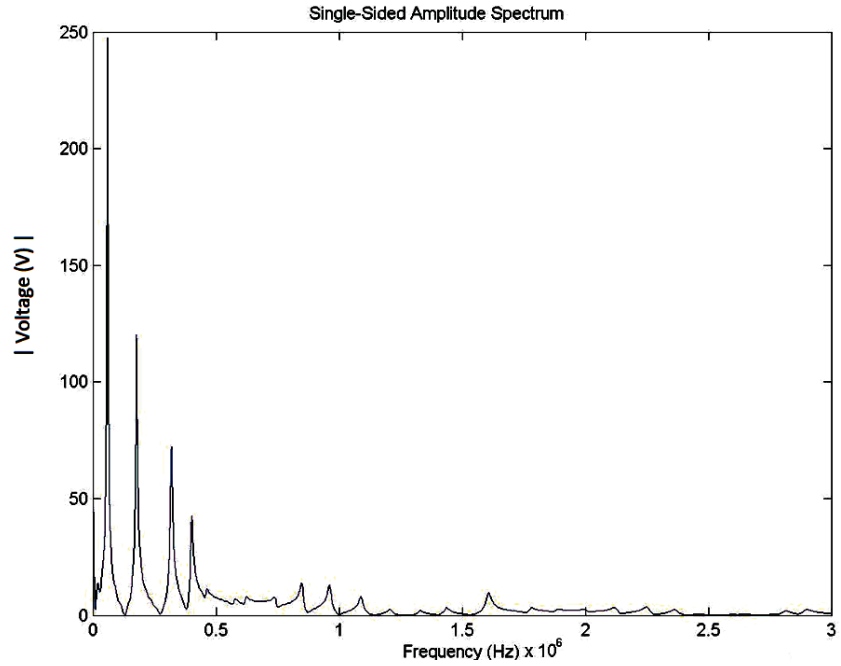

Figure 3.6 Frequency spectrum of voltage at 152.4 meter from Thumper, Point B

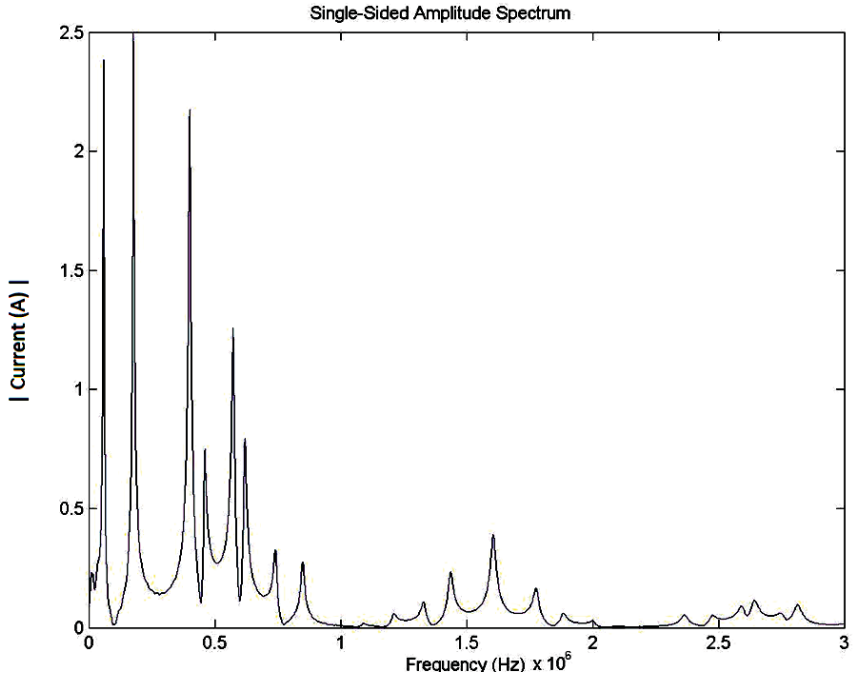

Figure 3.7 Frequency spectrum of current at 304.8 meter from Thumper, radial cable to transformer, Point C

3.3 Energized URD system model simulation and analysis

To obtain the characteristics of the transients of the test URD system provided by SDG&E, a typical 60 Hz, 12 kV, Energized URD system, (as shown in Fig. 3.8), was modeled in EMTP-RV. The model was simulated for different thumper voltage, thumper energy, different phase angle of power frequency at which the thumper is connected, thumper connected at various locations of URD, and system loaded at different loading conditions. By the results of these simulations, the characteristics of transients appearing on the URD upon thumper connections will be identified.

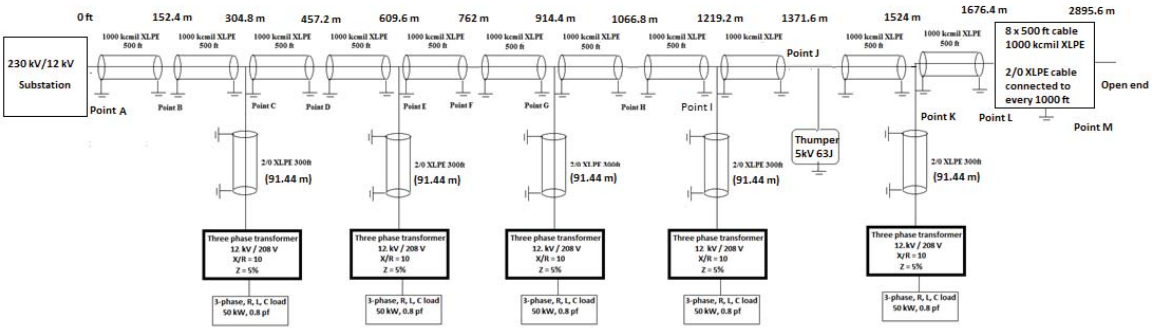

Figure 3.8 12 kV Energized URD system

The substation was modeled by step-down three phase transformers and three phase power source with source impedances representing the network beyond the substation. The load flow simulation was carried out prior to transient simulation to obtain the operating condition of the system. The substation bus was considered as slack bus for load flow simulation. Cables were modeled by frequency dependent modal transformation matrix model by EMTP-RV. Thumper was simulated by charged capacitor and triggered sphere gap. 3-phase 12 kV/208V was modeled based on the transformer equivalent circuit with non-linear inductance representing saturation

characteristics of flux in the core. 0.8 pf lagging loads were modeled as an R,L,C parallel circuit model. R, L, C values were based on the static loading condition.

3.3.1 Energized URD system model simulation for different thumper

The induced transients are different for thumping the URD with various thumper capacitance and voltage. Since the URD is energized and online, the safe thumper voltage should be evaluated. The thumper impulse will be super imposed on the power frequency waveform. The thumper energy and voltage should be small that the transients created do not interfere with the protection scheme of URD.

Simulations were run for the energized, lightly loaded URD system. Simulations were run for different thumpers as per Table 3.1.

Table 3.1 Different thumpers simulated for the energized URD

Thumper voltage (kV)	**Thumper Capacitance (µF)**	**Thumper Energy (J)**
5.2	0.1	1.352
5.2	1	13.52
5.2	5	67.6
5.2	10	135.2
7.5	0.1	2.8125
7.5	1	28.125
7.5	5	140.625

The simulations were performed for the thumper connected at Point ‘J’, 1371.6 meter from the substation end. Fig. 3.9 & Fig. 3.10 shows the time domain results for the 5.2 kV thumper. Fig. 3.11 & Fig. 3.12 show the time domain results for the 7.5 kV thumper. Fig. 3.13 shows the comparison of the waveforms of 5.2 kV and 7.5 kV thumper.

Fig. 3.9 and Fig. 3.11 show that the higher energy thumper produces transients which exist for more than 5 milliseconds. A thumper with capacitance more than 0.1 µF produces transients which changes the location of the peak of the power frequency voltage. Fig. 3.13 and Fig. 3.14 show that the increase in thumper voltage for the same thumper capacitance increases the magnitude of the peak values and does not affect the transient waveform oscillations. The thumper of 5.2 kV and 0.1 µF, 1.352 J was preferred for rest of the experiments.

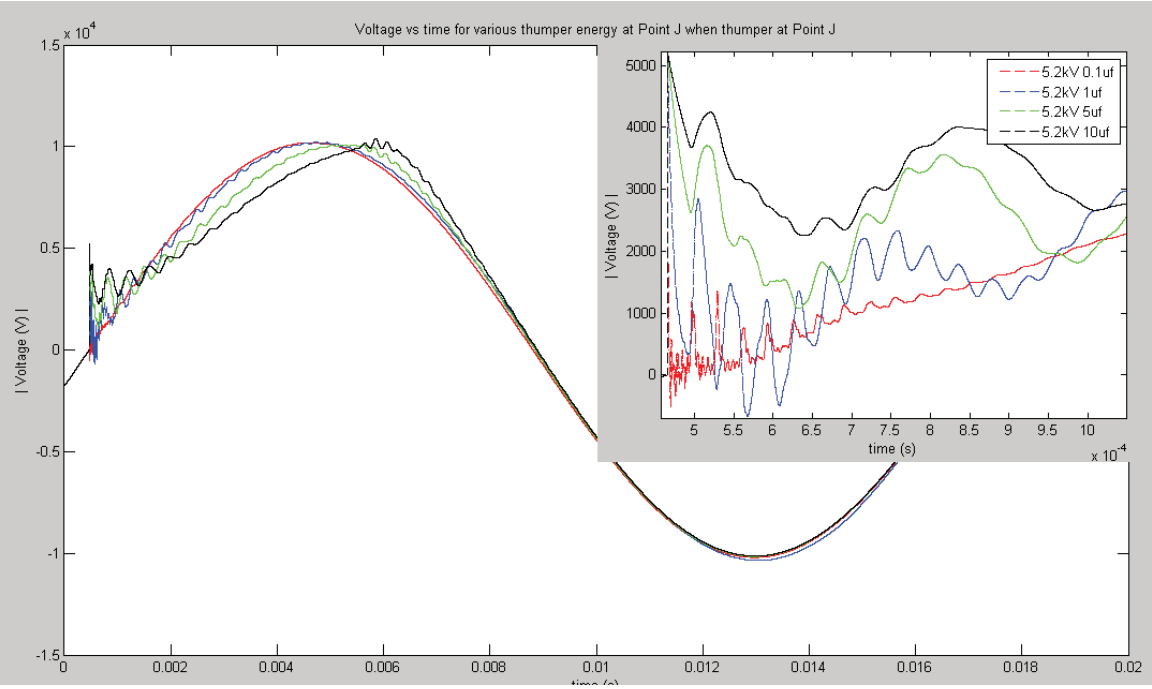

Figure 3.9 Voltage function time for 5.2 kV thumper voltage and 0.1 µF, 1 µF, 5 µF & 10 µF thumper capacitance

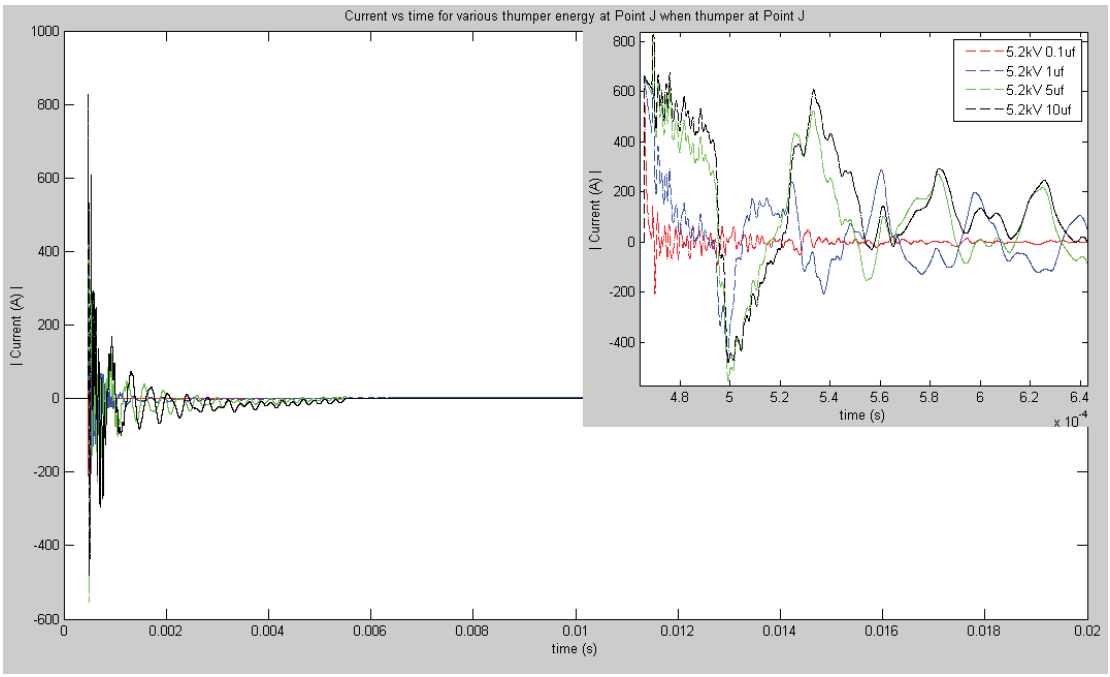

Figure 3.10 Thumper current function time for 5.2 kV thumper voltage and 0.1 µF, 1 µF, 5 µF & 10 µF thumper capacitance

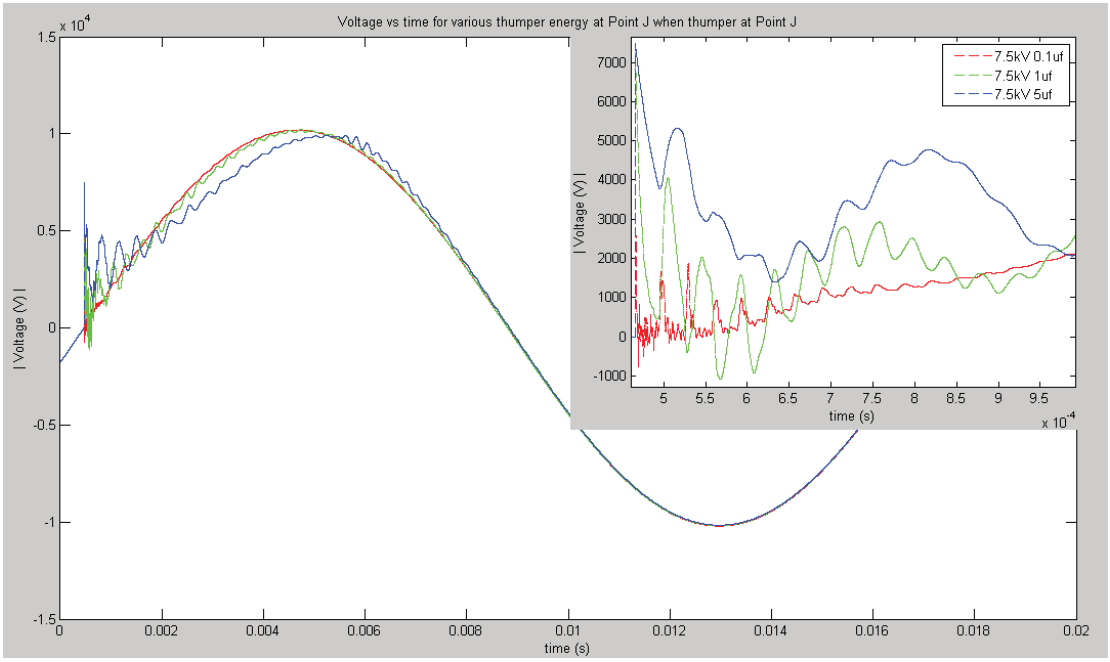

Figure 3.11 Thumper voltage function time for 7.5 kV thumper voltage and 0.1 µF, 1 µF, 5 µF thumper capacitance

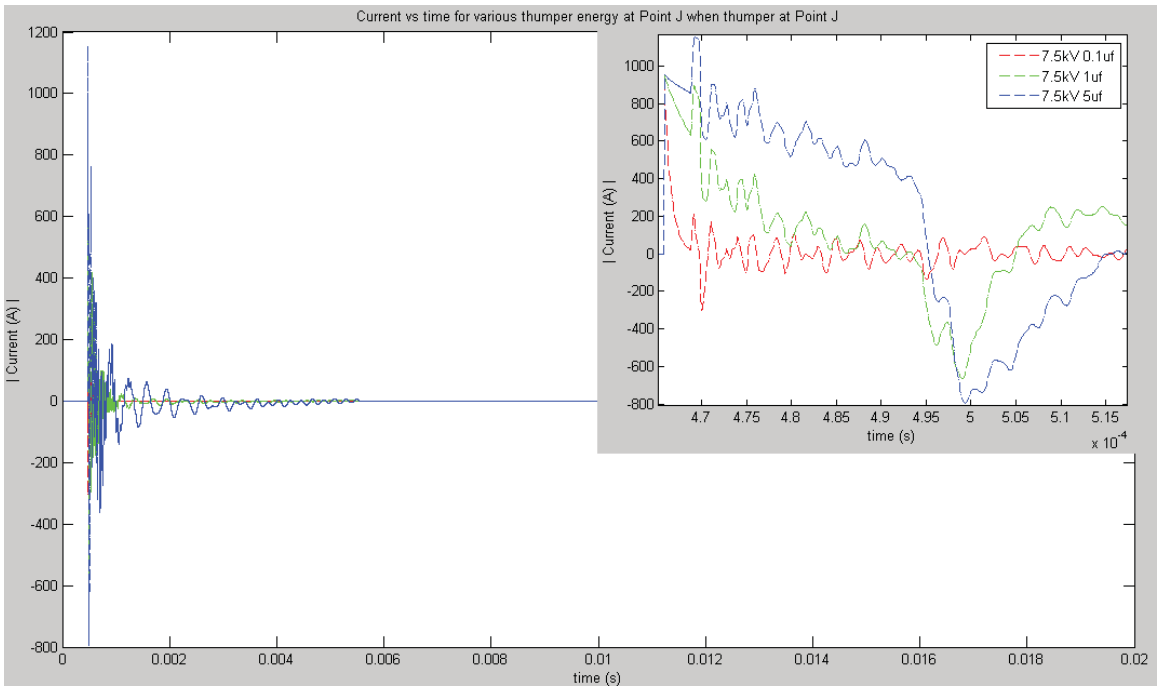

Figure 3.12 Thumper current function time for 7.5 kV thumper voltage and 0.1 µF, 1 µF, 5 µF thumper capacitance

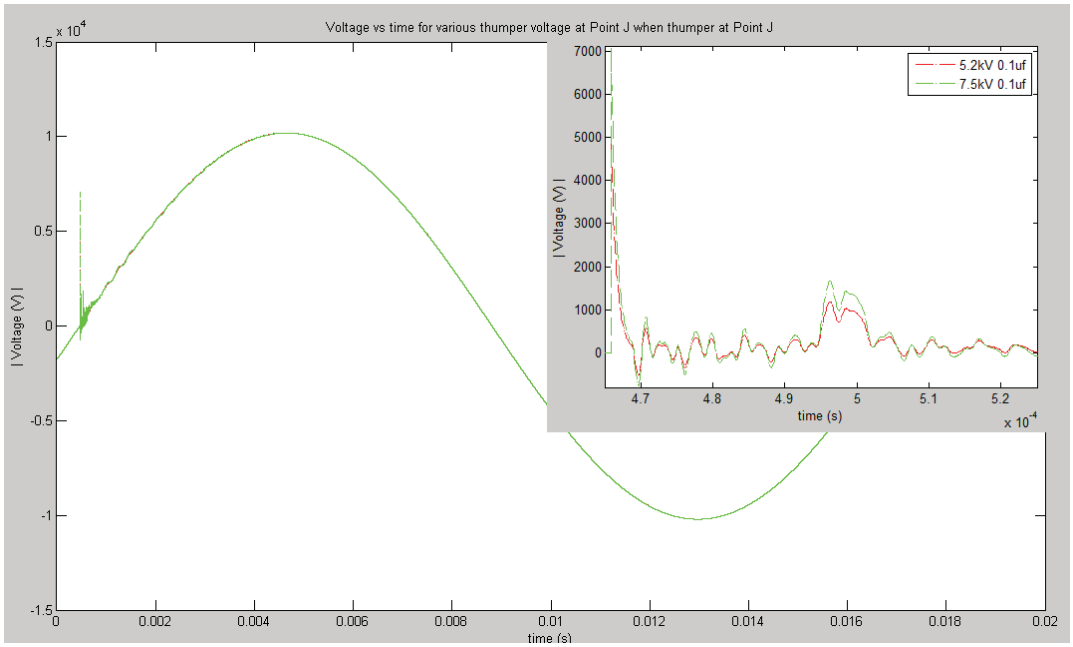

Figure 3.13 Thumper voltage function time for 5.2 kV & 7.5 kV thumper voltage and 0.1 µF thumper capacitance

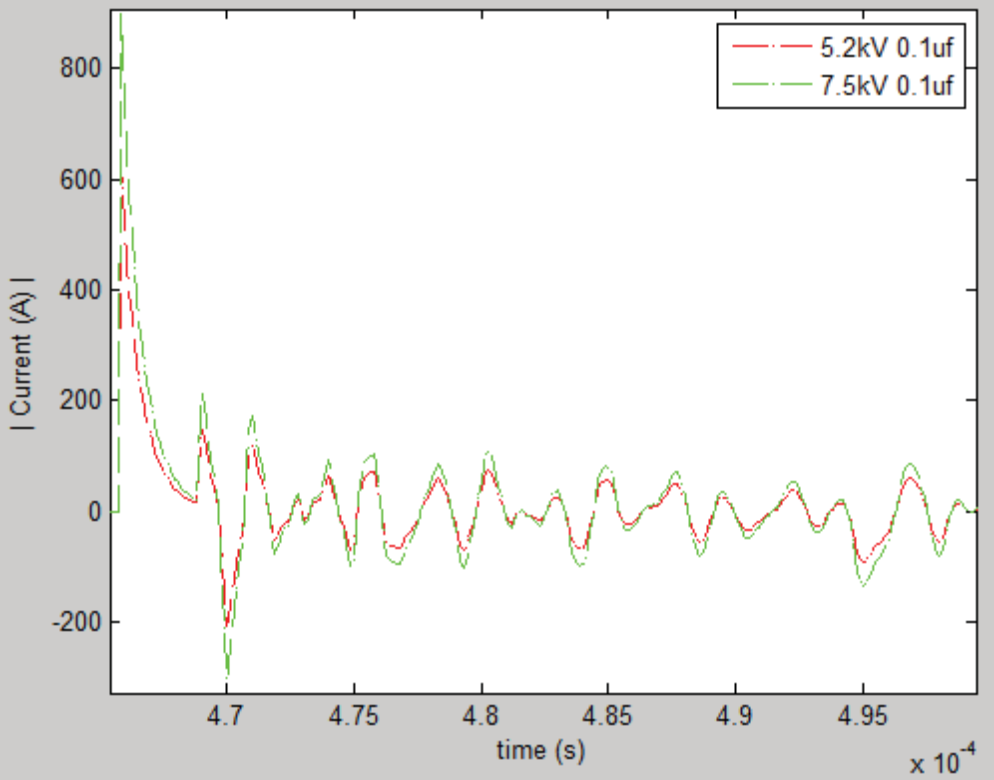

Figure 3.14 Thumper current function time for 5.2 kV & 7.5 kV thumper voltage and 0.1 μF thumper capacitance

3.3.2 Energized URD system model simulation for different phase angle triggering

Induced transients are different when the thumper is connected at different angle of power-frequency. To find out best way to trigger the thumper, simulations were run for energized, lightly loaded URD system, as shown in Fig. 3.8. Simulations were run for 5.2 kV, 0.1 μF thumper connected during the different phase angle of the power frequency at the place where thumper was connected.

Fig. 3.16 & Fig. 3.17 show the time domain waveform at point 'J' due to firing the same energy thumper at different phase angle of the power frequency. Fig. 3.16 shows that the peak voltage that appears at the thumper place is roughly 12 kV (for negative cycle) for all the cases of simulation. Fig. 3.17 shows that the peak current

depends upon the difference between the voltage of the thumper and the voltage of URD at which the thumper is connected. The peak thumper current is 1900A momentary. The steady state current which would be seen in the thumper due to capacitive load may reach a value of 0.5Arms maximum. As the triggering angle changes, the voltage and current transient duration changes, but the changes are very minimal for 15 degree and 0 degree. The transient duration lies within 5 ms for 15 degree and 0 degree of operation. The transient time of 30 degree is very small due to the large reduction in the transient's magnitude, as seen by the small green transient in Fig. 3.16 and Fig. 3.17. This is same for all the cases when the thumper is trigged at the power cycle voltage closer to the thumper voltage.

Fig 3.15, frequency spectrum, shows that the obtained frequency response was amplitude scaled. The frequency domain results of all the simulation cases have the same frequency content with amplitude scaling.

The voltage and the current transient duration changes depending upon the difference between the power frequency instantaneous voltage and thumper charged voltage. Thumping at zero (0) degree to 10 degree of power frequency is ideally preferred. If the difference in the voltage is less than 2 kV, measurement and recording of the transient would be difficult. Hence, recording measurements while connecting the thumper when power frequency will be at 15-45, 135-165 (positive thumper) and 195-225 and 315-345 (negative thumper) degree are not preferred. These angles correspond to power frequency voltages of magnitude very close to that of thumper voltage and correspond to 16% of time period of power frequency.

These observations suggest that a power frequency angle specific thumper connection, which is an expensive complex system and expensive, is not necessary, but at

the same time recording frequency domain impedance information. Thumping at any of the 84% of the power frequency produces the same results, which can be scaled during signal processing.

Additional results of captured time domain and frequency domain results are presented in Appendix C.1.

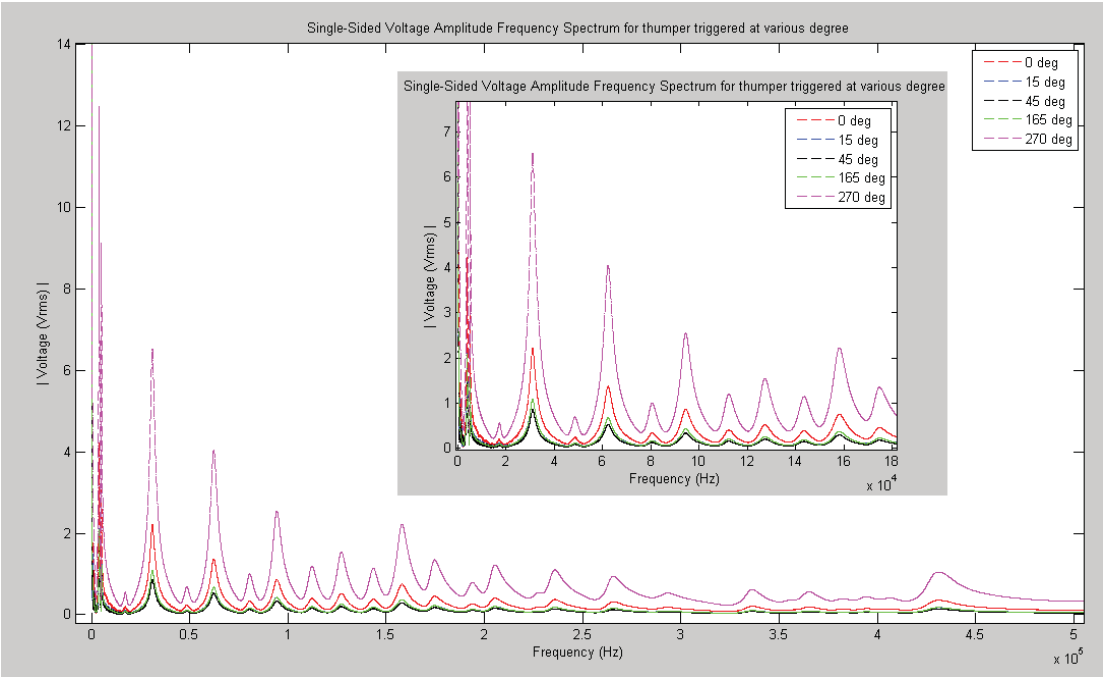

Figure 3.15 Single-Sided Voltage Amplitude Frequency Spectrum for Thumper triggered at various phase degree of power frequency

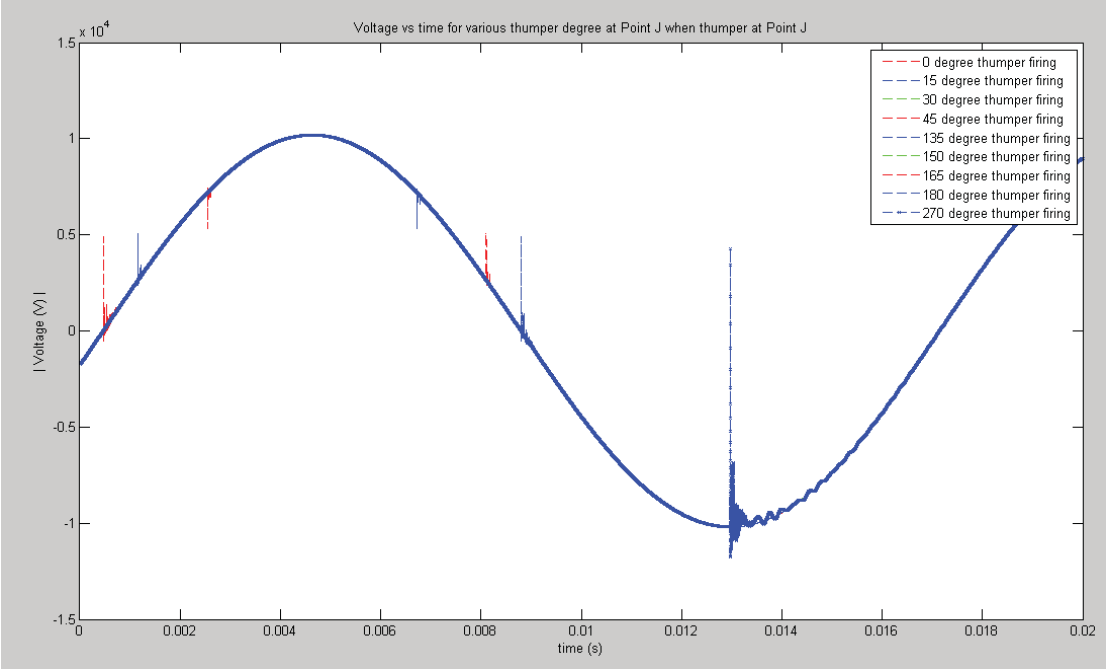

Figure 3.16 Voltage function time for various thumper degree at point 'J' and triggered at various phase degree of power frequency

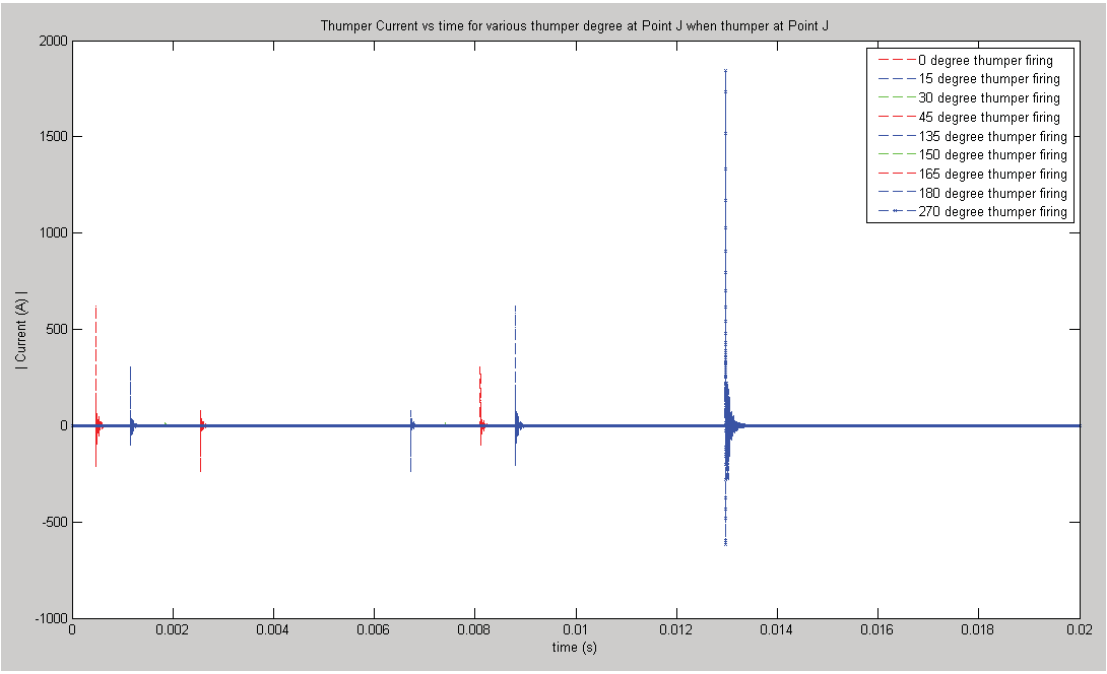

Figure 3.17 Thumper current function time for various thumper degree at point 'J' and triggered at various phase degree of power frequency

3.3.3 Energized URD system model simulation for different positions of URD

In order to observe the transients appearing along the URD, simulations of the URD are carried out for 5.2 kV, 0.1 μF thumper. The thumper is varied at 7 positions along the URD length. Simulations were run for the energized, lightly loaded URD system, as shown in Fig. 3.8. The least energy thumper (5.2 kV, 0.1 uf, 1.352 Joule) is considered to observe the effect of attenuation as the thumper moves away from Point 'J' to either side of Point 'J'. Voltage and current are observed at the midpoint of the URD. The power frequency sinusoidal signal was removed from the voltage and current waveform and is presented in Fig. 3.18 and Fig. 3.19. The waveform presents the peaks in a time domain graph, showing the time at which the reflected wave from either side is observed.

Fig 3.20 shows the attenuation of the impulse as it travels along the length of the URD every 152.4 meter. Fig. 3.18 & 3.19 shows that the peak voltage magnitude and current of transients were reduced by 1kV and 70 A as the thumper is moved 152.4 meter away from the observation point. The peak value is reduced by 1.9 kV and 120 A when the thumper was moved to 1371.6 meter away from the cable. For thumper at 1371.6 meter, as shown by the black line in Fig. 3.18, voltage amplitude for every reflected waveform has attenuated from 3.8 kV at source to 1 kV after travelling 2743.2 meter. The signal is attenuated by 30% as it reaches 152.4 meter. Additional results of captured time domain and frequency domain results are presented in Appendix C.2.

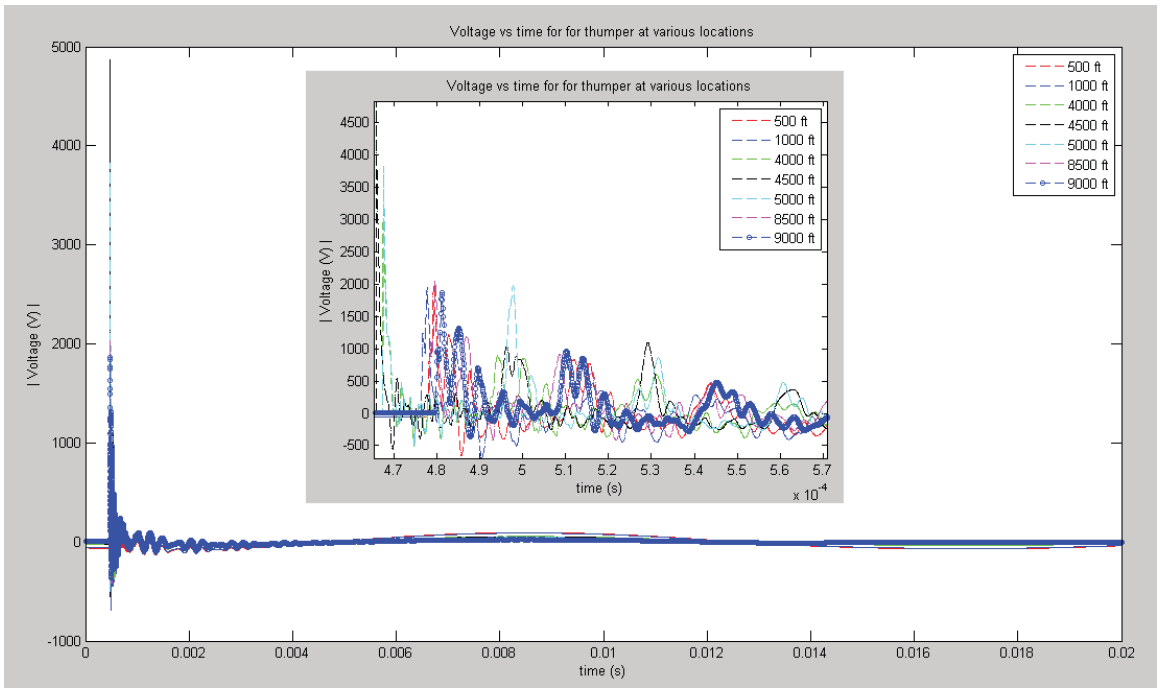

Figure 3.18 Voltage function time for Thumper at Various Locations

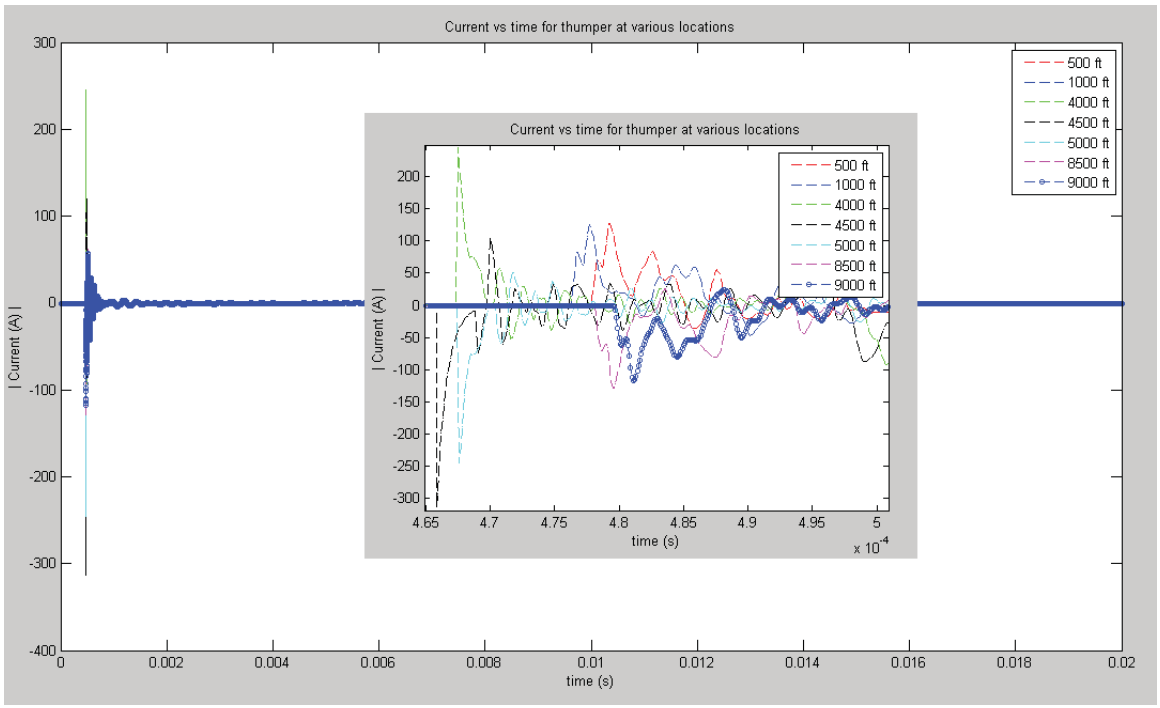

Figure 3.19 Current function time for Thumper at Various Locations

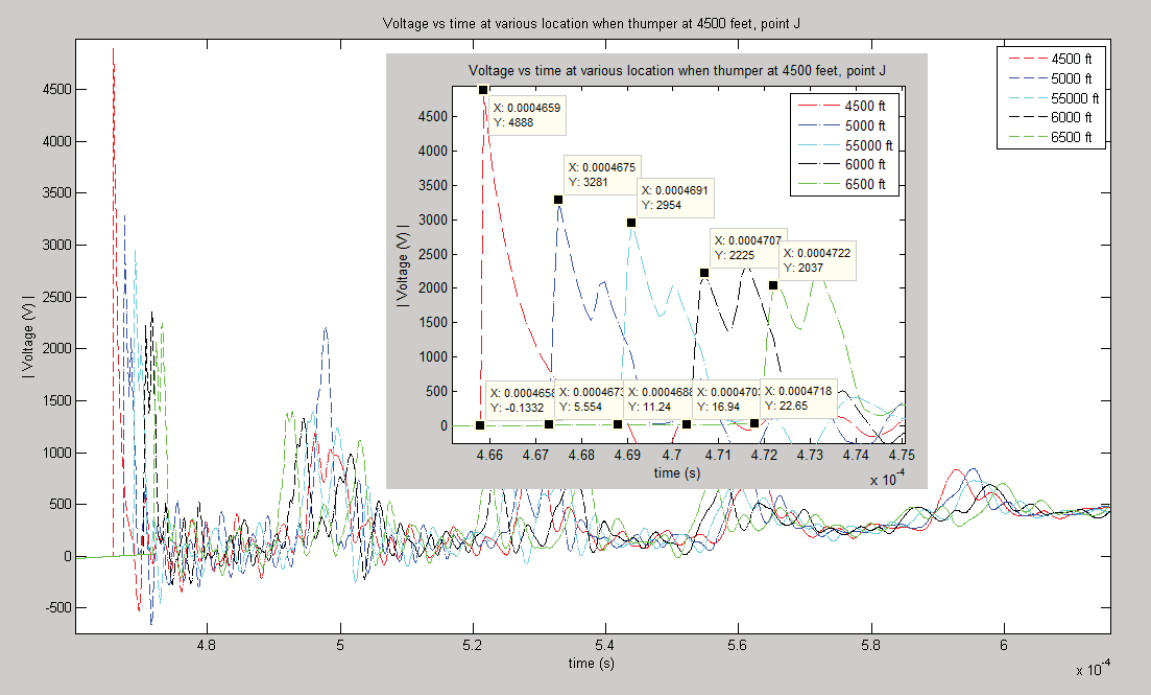

Figure 3.20 Voltage function time at various locations 152.4 meter apart

3.3.4 Energized URD system model simulation for different loading conditions

The simulations were run for the energized system to observe the effect of loading conditions. Uniform and non-uniform loading conditions were chosen based on the ampere rating of the cable. The rated current capacity of the main feeder is 600 A, and the radial feeder is 200 A. Table 3.2 and 3.3 show the different loading conditions cases. In simulation, 5.2 kV, 0.1 µF thumper was connected at zero crossing of power frequency of the voltage at point 'J'.

Table 3.2 Simulation of uniform loading conditions

Loading condition	Main feeder current (A, rms)	Radial feeder current (A, rms)
Light loading	**25**	**3**
Medium loading	**250**	**29**
Heavy loading	**436**	**50**

Table 3.3 Simulation of Non-uniform loading conditions

Loading condition	Main feeder current (A, rms)
Non-uniform loading case 1: Heavy Load concentrated on point 'M', rest of the transformers are lightly loaded.	**65**
Non-uniform loading case 2 : Heavy Load added to case 1 at 152.4 meter from point 'M'	**187**
Non-uniform loading case 3 : Heavy Load added to case 2 at point 'K'	**229**

Fig. 3.21 and Fig. 3.23 show the voltage and thumper currents at point 'J' for different uniform loading conditions. Fig. 3.22 and Fig. 3.24 show the voltage and thumper currents at point 'J' for different non-uniform loading conditions. Fig. 3.21 and 3.22 show that the loading of the URD system does not significantly affect the voltage transient magnitude or duration.

Fig. 3.23 and 3.24 show that the loading the URD system does not significantly affect the thumper current transient magnitude or duration.

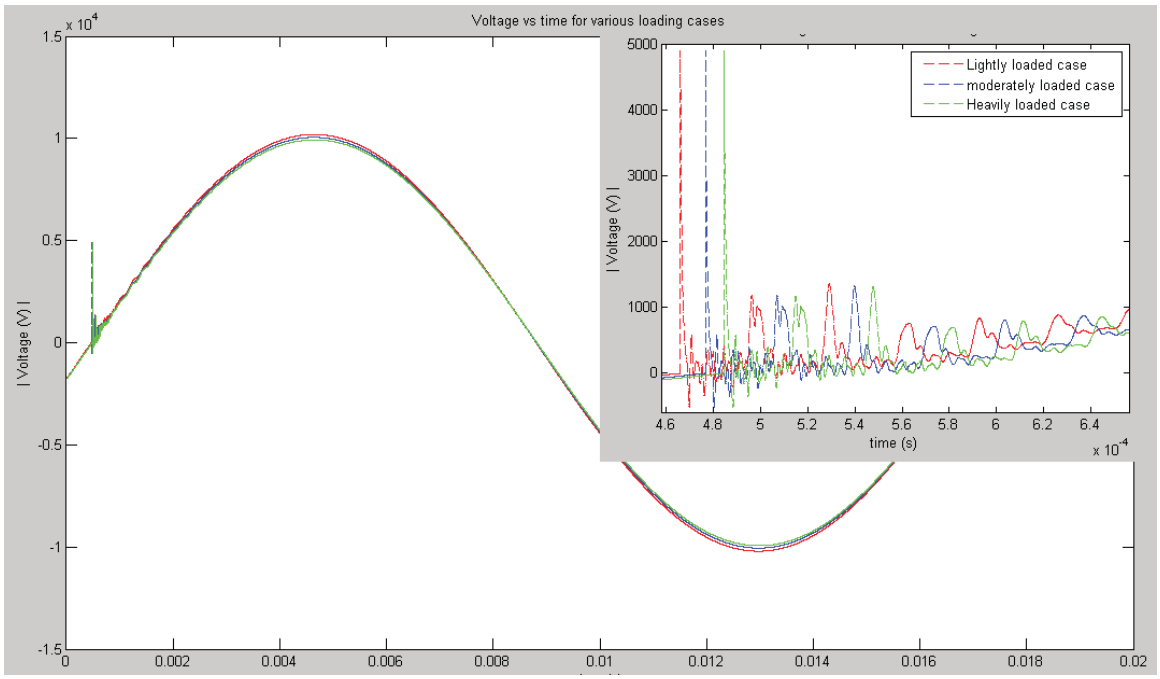

Figure 3.21 Voltage function time for three types of uniform loading system

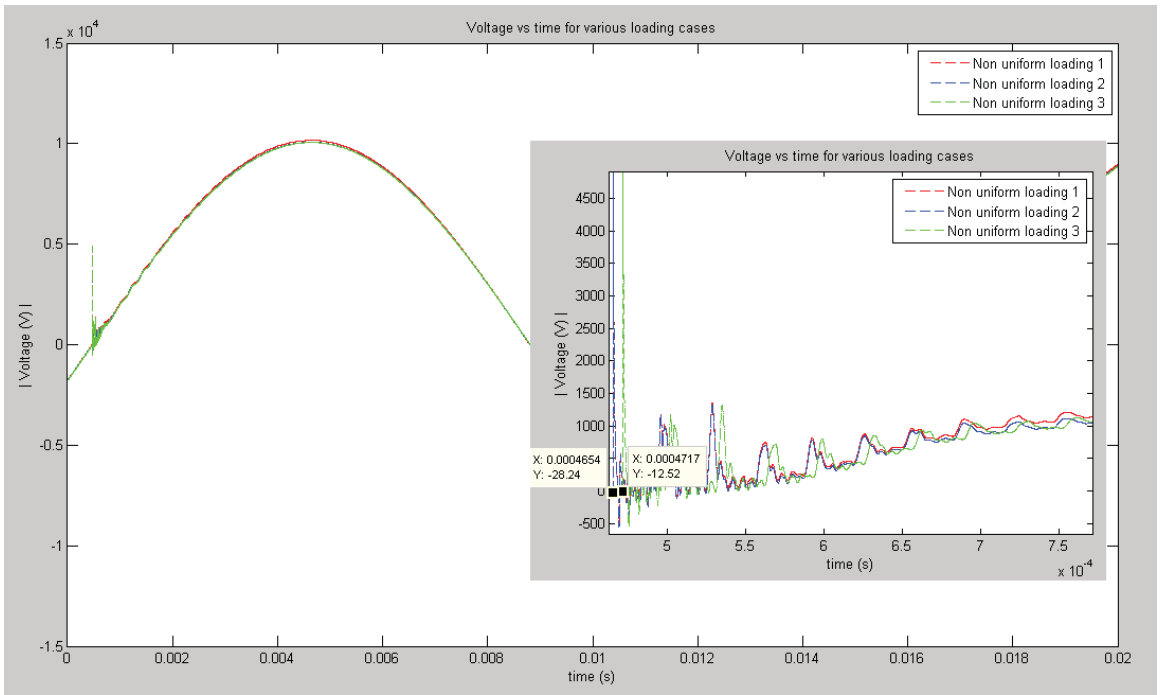

Figure 3.22 Voltage function time for three types of non-uniform loading system

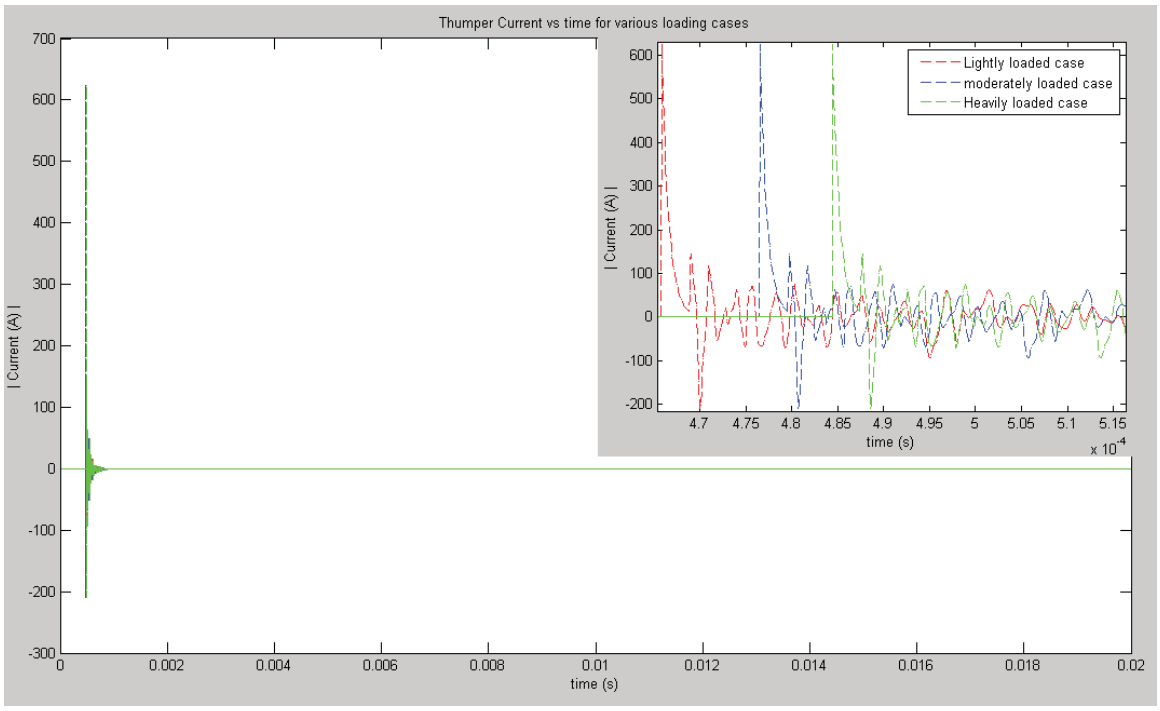

Figure 3.23 Thumper current function time for three types of uniform loading system

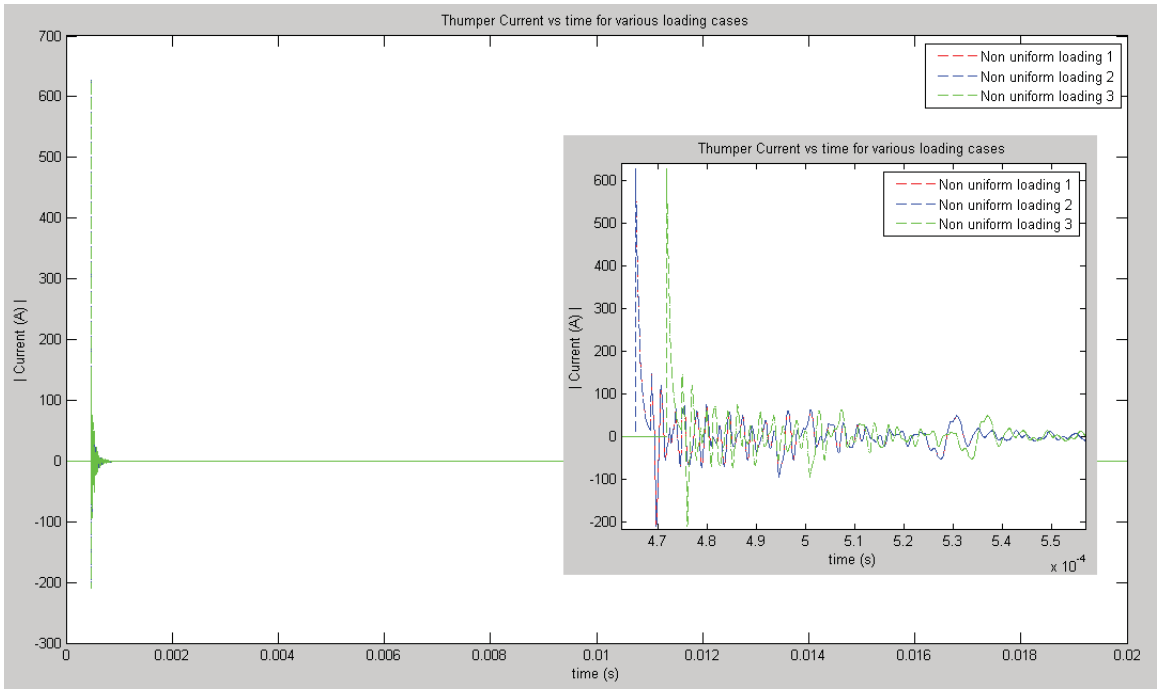

Figure 3.24 Thumper current function time for three types of non-uniform loading

Fig. 3.25, 3.26, 3.27, and 3.28 show the incoming cable end current and outgoing cable end current at the junction of thumper and cable feeders. From Fig. 3.25, 3.26, 3.27, and 3.28, it is clear that loading the URD system introduces power frequency bias to the transients. When the power frequency current is removed from the response using MATLAB, the transients are the same for different loading conditions. This effect could be explained by the decoupling of the primary feeder network from the load by transformer for impulse voltages and currents. There are time shifts in these waveforms, which are due to the shift in triggering simulation time for different loading conditions due to phase angle changes of the bus voltage with respect to source voltage as reference.

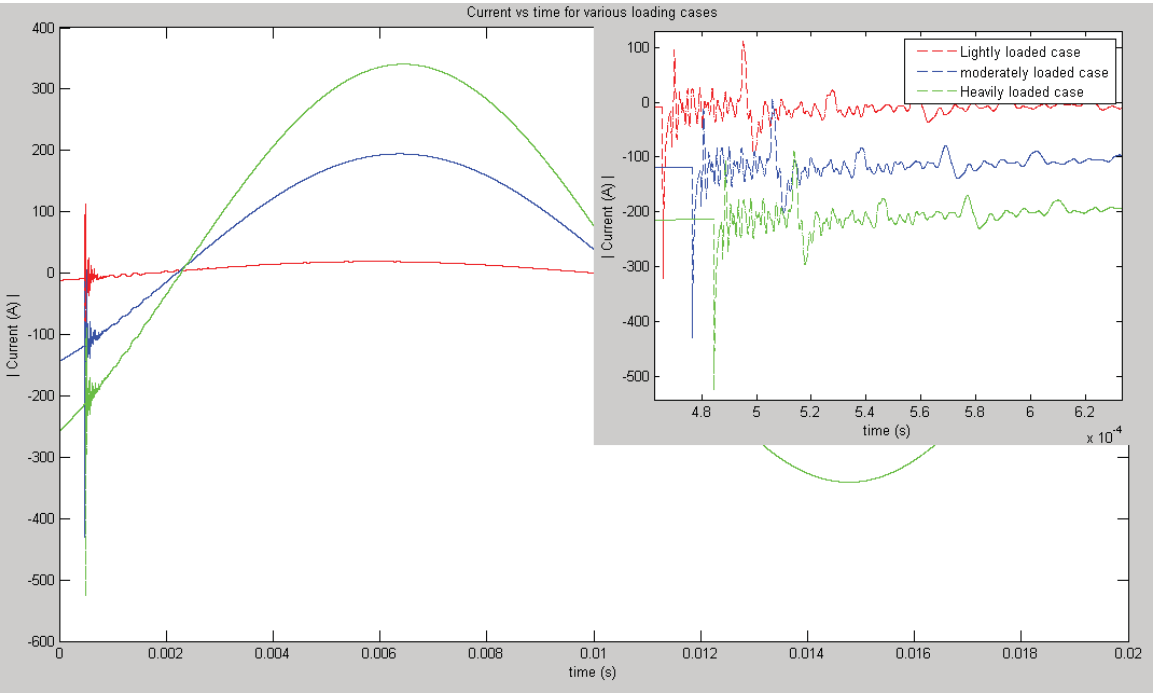

Figure 3.25 Current function time at incoming cable end for three types of uniform Loading

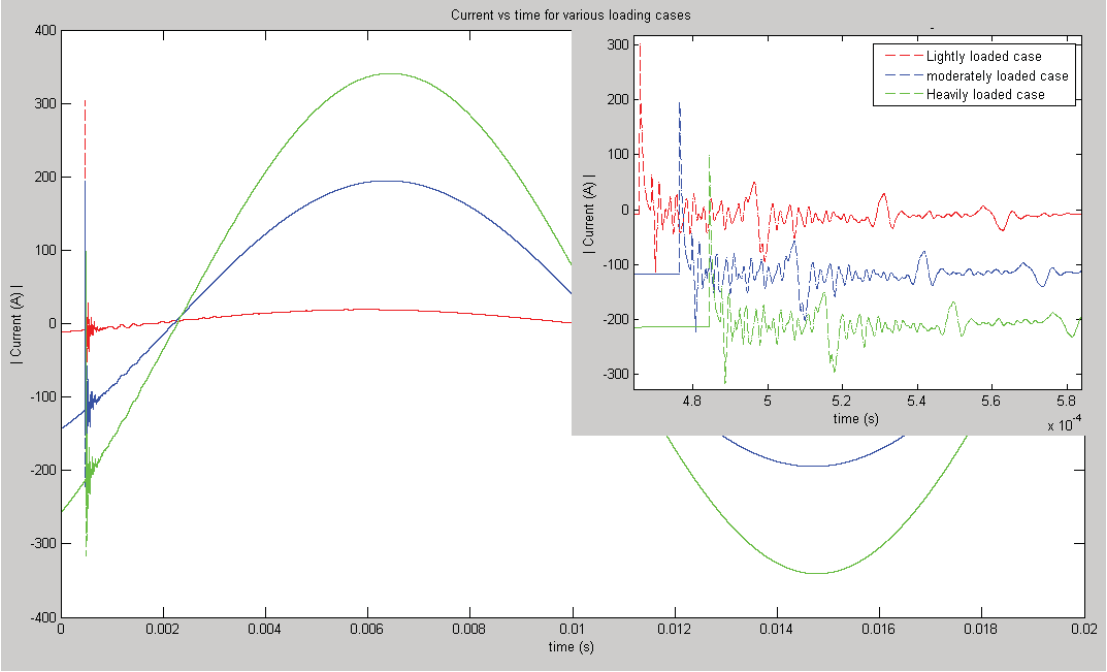

Figure 3.26 Current function time at outgoing cable end for three types of uniform loading

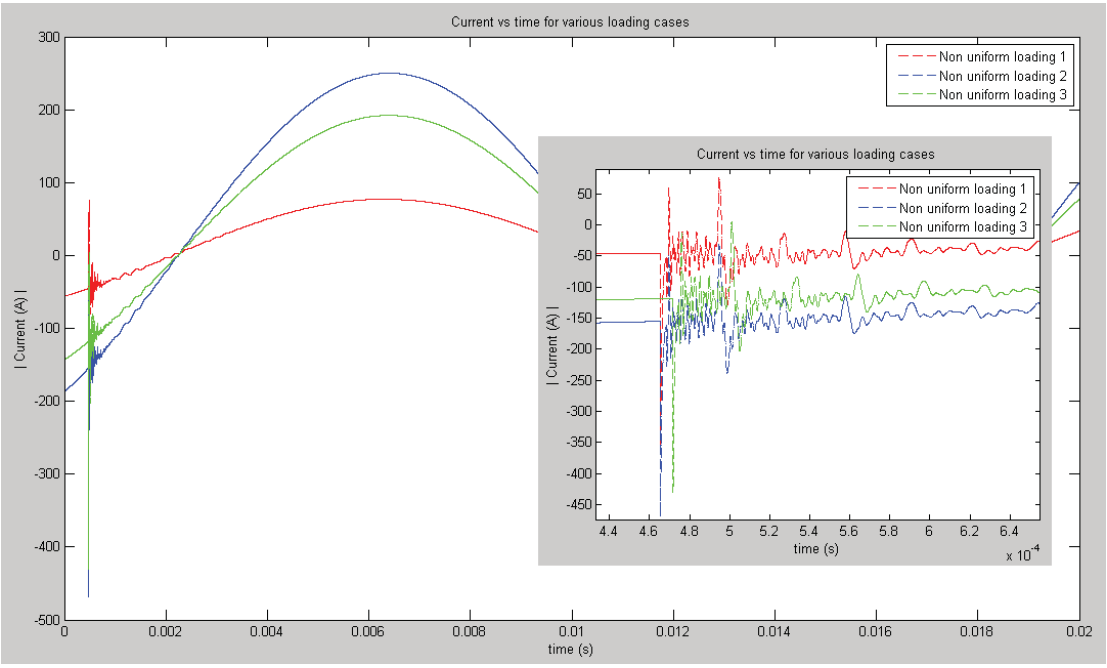

Figure 3.27 Current function time at incoming cable end for three types of non-uniform loading

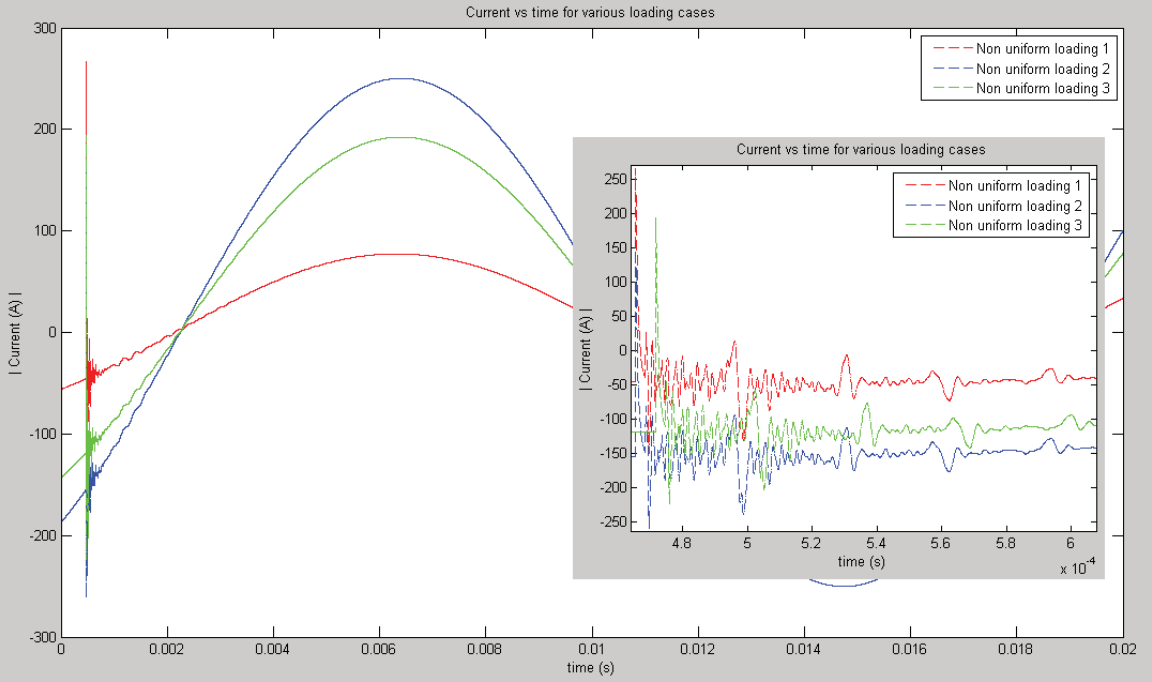

Figure 3.28 Current function time at outgoing cable end for three types of non-uniform loading system

3.3.5 Energized URD system model simulation for differential measurements

During wide spread implementation of the recording devices, differential measurements of URD, measurements taken in two or more different locations, are preferred to improve noise immunity. In order to record transients in different locations, the recorders should be either external triggered for synchronous measurements, or should be signal triggered for non-synchronous measurements.

Simulations were carried out to find the response obtained for synchronous and non-synchronous method of recording of transients. Voltages at various places along the travel of the URD were recorded during the simulation of the energized URD for light loaded condition and when thumper is connected at Point J The synchronous method of transient recordings from simulations were time shifted to get self triggered non-synchronous waveform. From Fig. 3.29 and Fig 3.30, the effect of matching

waveform with reflected wave from either end was seen in both synchronous and non-synchronous measurement.

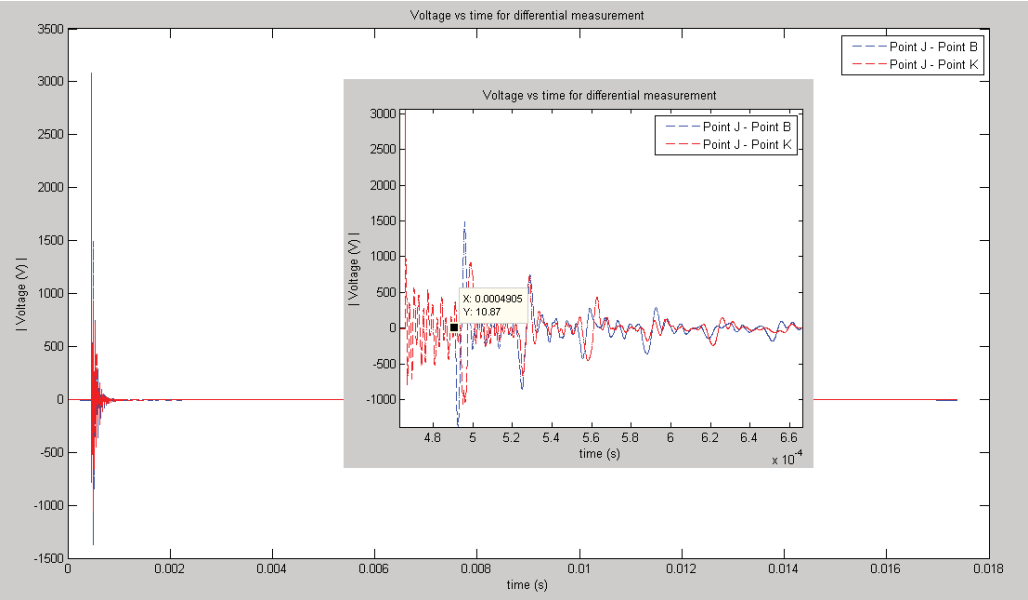

Figure 3.29 Differential Measurement (V vs t) with the measurement on either side of thumper, (Point B and Point K) shifted in time to represent non-synchronous differential measurement

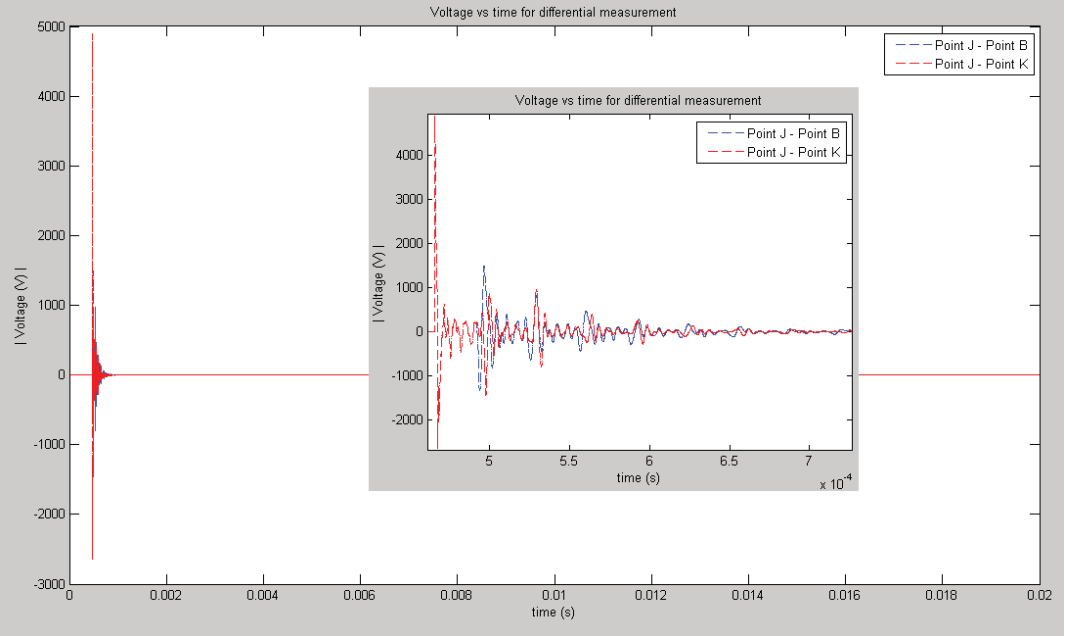

Figure 3.30 Differential Measurement (V vs t) with the measurement on either side of thumper (Point B and Point K) not shifted in time to represent synchronous differential measurement

Both non-synchronous and synchronous measurement captures the transients. Synchronous triggering of recording system takes additional recording time and recording of more insignificant power frequency waveform prior to appearing transient impulse. Time-stamped non-synchronous recording could be extended by power frequency and can produce the same results of synchronous recording. Signal dv/dt triggering gives optimal use of recording instrument. Additional results of captured time domain and frequency domain results are presented in Appendix C.3.

3.4 Quantization signal to noise ratio (SNR) level to determine the vertical resolution

Transient recorder noise level due to LSB error was identified by Signal to Noise Ratio (SNR) of the quantizer used. Floor and hold quantizer were used in this study to find the vertical resolution of the recording instrument. Table 3.4 & Table 3.5 shows the

SNR for number of bits from 10 to 22. The full scale value of 15 kV and 1000 A was considered for quantization of the transient current signal. The difference in the quantized waveform and the actual waveform gives the error associated with quantization. Fig. 3.31 & Fig. 3.32 show the quantization error for voltage and current respectively.

From the Fig. 3.31 & Fig. 3.32, as the vertical resolution (number of bits used per sample) was increased, the error drastically reduces from 10 bit to 14 bit. 16 bit is selected for vertical resolution.

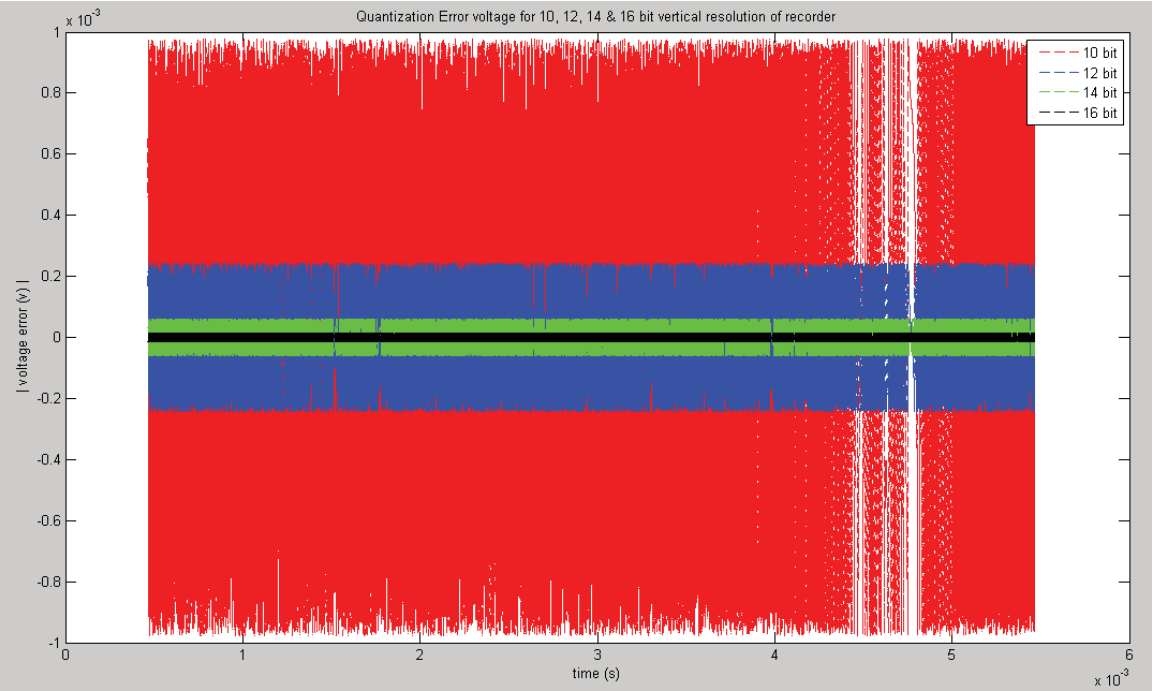

Figure 3.31 Quantization error voltage for 10, 12, 14 & 16 bit vertical resolution of recorder

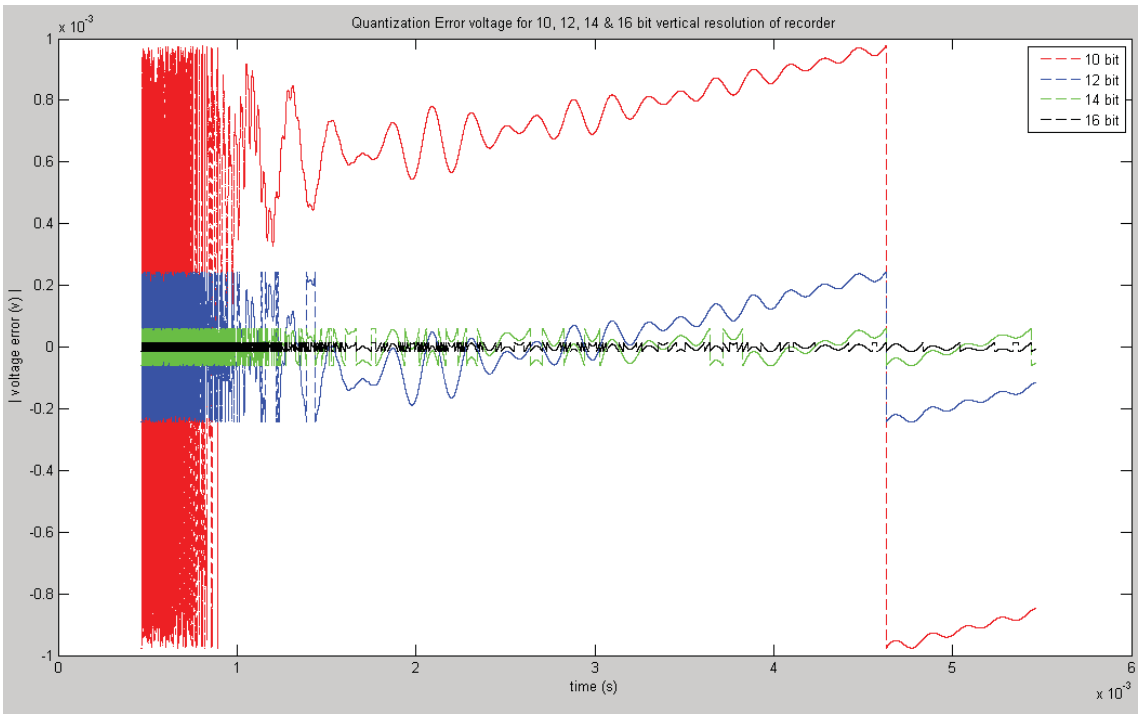

Figure 3.32 Quantization error current for 10, 12, 14 & 16 bit vertical resolution of recorder

Table 3.4 Signal to Noise Ratio (SNR) due to floor quantization for voltage and current at thumper

No of bits	SNR of voltage	SNR of thumper current
10	62	19.7
11	68	27.4
12	73.97	34.76
13	80	40.4
14	86.037	46.63
15	92	52.5
16	98.04	58.7
17	104	64.68

Table 3.5 Signal to Noise Ratio (SNR) due to round quantization for voltage and current at thumper

No of bits	SNR of voltage	SNR of thumper current
10	76.7	16.2
11	82.7	21.26
12	88.76	28.44
13	94.79	34.77
14	101	40.02
15	106.8	46.65
16	112.85	52.71
17	118.87	58.65

3.5 Attenuation in cable

The sample cable as shown in Fig. 2.1 of Section 2 examines the attenuation issues of the cable. The travelling wave equations of Eq. 2.2 – 2.6 were used to calculate the propagation constants. The attenuation at each length was plotted for all the frequencies up to a length of 3600 meter. The cable was considered infinitely long and did not have any bifurcation for the entire length. Fig 3.33 shows the attenuation in percentage, i.e. the percentage of signal attenuated for any length of the cable and frequency, 0% meaning un-attenuated signal. 100% meaning no signal was completely attenuated.

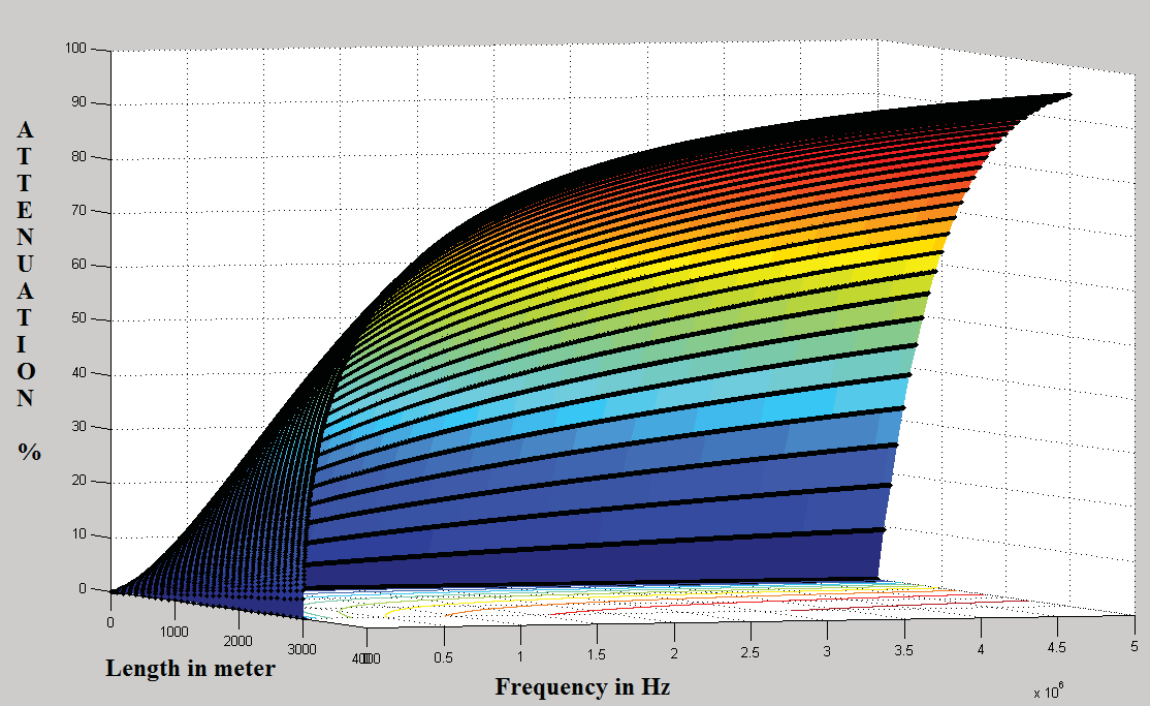

Figure 3.33 Percent attenuation of signal of different frequency over the length of the cable (up to 3048 meter)

The maximum distance from the point of pulse source, thumper, which has a good signal, was calculated based on dBV of attenuation. Thirty percent voltage magnitude attenuation corresponds to -3dBV.

Hence the frequencies which gets attenuated more than 30%, -3 dBV at each length of the cable are plotted to have a better understanding of the signals which will be measured from a greater distance from the source. Since in an URD system, the signals were getting reflected, this helps us to analyze the signal with reflections. Fig 3.34 shows length on y-axis and the frequency at each length which gets attenuated to -3 dBV.

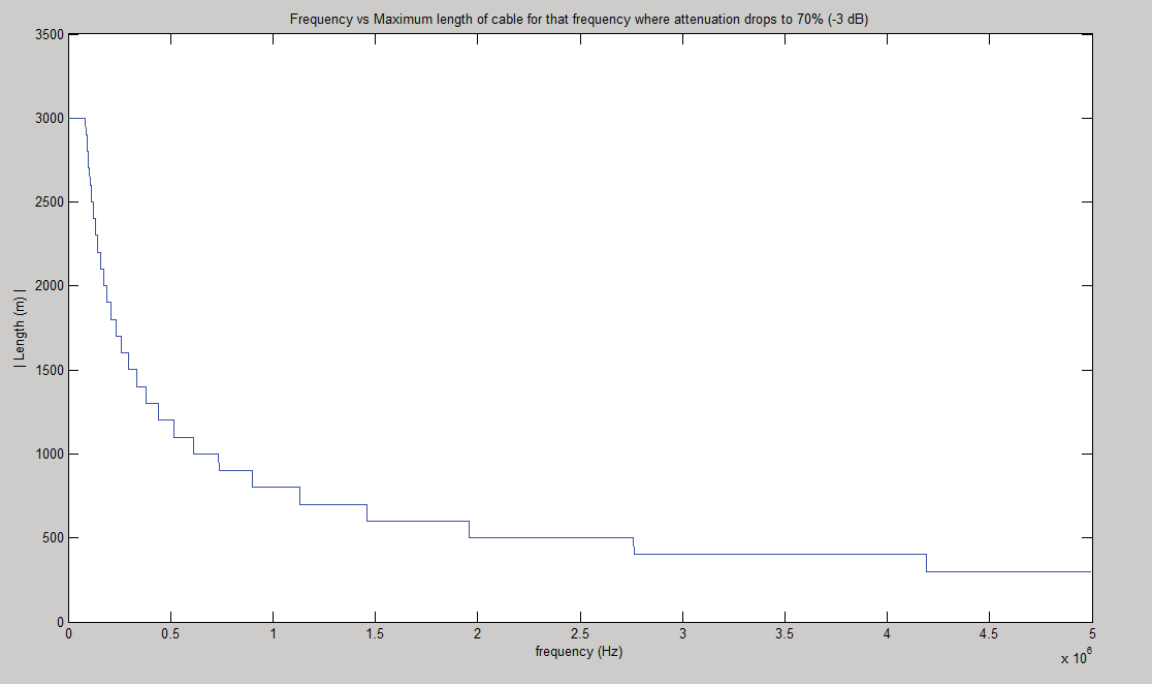

Figure 3.34 Frequency vs Maximum length of cable for that frequency where signal amplitude drops by 30% (-3 dBV)

CHAPTER IV

PROPOSED MEASURMENT METHODOLOGY

The measurement system consists of two parts. The first system is the thumper system. It is the source of induced transients, consists of a charged capacitor connecting to URD with protective devices. The second system is the measurement system. It consists of dividers and transformer, matching cables, and signal amplifiers with protective system. The details of these components are presented in following sections.

4.1 Thumper system

- Based on analysis of induced transients by various thumper voltage and energy, a thumper of capacitor specification 5.2 kV, 0.1 μF, 1.352 J is selected to induce transients in SDG&E Radial URD system.
- A safely grounded panel with rollers is selected to be used to house multi tap bus, the main circuit breaker and its protection relay, vacuum contactor, high frequency current transformer, control buttons for breaker and contactors, and power indicator lights. Fig. 4.1 shows the diagram of overall schematics of thumper and measurement system.
- A safety Main Vacuum Circuit breaker (MB) for 15-20 kV with over current and over voltage relays, with supporting PT and CT is selected. The purpose of the main breaker is safety breaker for fault conditions within thumper system. This breaker should also be capable of manual/remote input operation.

- The thumper power frequency follow up current after switching transients has a value of less than 1A. A 15-20 kV vacuum contactor (C-A) with breaking capacity of more than 2A, trip relay and fuse arrangement is selected to break the circuit. A typical vacuum circuit contactor can break the circuit within three cycles of power frequency after the signal is delivered to its trip relay. So, high speed vacuum contactors/relays, which can break within 1 power cycle, once the relay is triggered to open is selected for the purpose.
- Multiway cable taps are selected to connect the thumper side measurement system, if there are no tap points available on the URD for the measurement system.
- A high frequency current transformer (HFCT), a part of measuring system, is selected to install in the thumper panel to measure the thumper current.
- Control switches and buttons for breaker and contactor and light indicators are selected to install into the main panel.
- Trigger signals will be generated from thumper and will transmit to main panel vacuum contactor relay to signal opening of vacuum contactor.
- Cable load break elbows of 200A is selected to be used to connect the multi tap bus in mobile panel to URD grid [11].

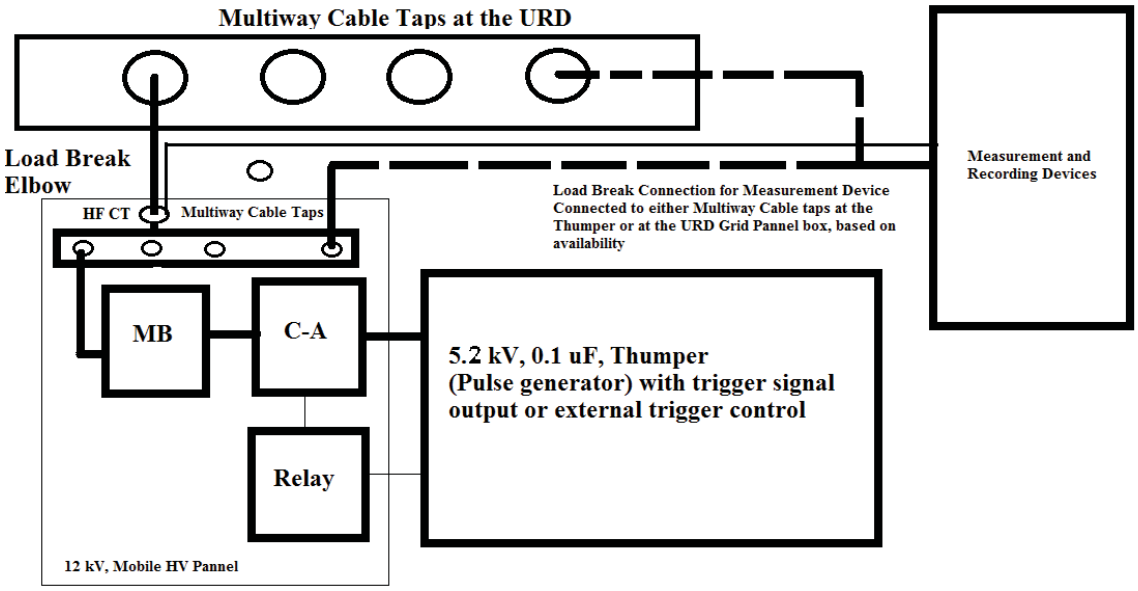

Figure 4.1 Thumper connection circuit details

4.1.1 Thumper operation

- Based on analysis, operating the thumper at phase angle degree other than 15-45, 135-165, 195-225, and 315-345 is selected. This phase angle interval counts for 16% of power frequency time. Measurements at 84% time period of the power frequency produce scaled frequency response. Hence measurements are repeated until the recorded transient peak voltage value is more than 2 kV.
- Based on the measurement system recording, during signal processing, the recorded transients is selected to be time shifted and scaled to remove the effect of power frequency bias and scaling.

4.1.2 Thumper connection sequence

1) Breakers, contactors, and thumpers are to be open prior connecting the thumper to the URD.

2) The thumper is to be charged to required voltage (5.2 kV) and the charging DC source of the thumper capacitor is to be disconnected from thumper capacitor by internal DC source thumper contactor.

3) The Main Breaker (MB) is to be turn on allowing voltage from grid to pass onto the vacuum contactor.

4) The contactor (C-A) is to be closed allowing power from grid to be available at the thumper end.

5) The thumper can now be manually/electronically triggered to close the thumper contactor to make the circuit. This will create transients which propagates in URD.

6) A 5 ms delay timer is selected to send open signal to contactor (C-A). C-A will break the circuit and the thumper will be isolated in 1 – 3 power frequency cycles.

7) Main circuit breaker is to be turned off and thumper can be physically disconnected by using load break elbows.

4.2 Measurement system requirements

- On the basis of analysis, the voltage and current dividers are selected to have a minimum bandwidth of 2-3 MHz and switching BIL same as that of the URD system The specifications of recording instruments in [40, 13] also has similar bandwidth.
- From the analysis and frequency spectrum of voltage and current measurement, the minimum sampling rate, as per Nyquist criteria, of 4-6 MS/s is chosen for transient recorder.

- From the analysis of simulation, the maximum transient duration is found to be 5 ms. The recording instrument should have sweep time of 5 ms. Therefore the transient recording instrument is selected to record 20000-30000 (32768) samples @ 4-6 MS/s.
- Analysis revealed that signal to noise ratio (SNR) of recording instrument for 16 bit vertical resolution is greater than 60 dBV. 16 bit of vertical resolution is selected based on simulations. This demands 32 kb of memory of 16 bit resolution @ 6 MS/s.
- Non-synchronous, dv/dt triggering is selected for transient recorders to enable differential measurements at various points in cable. Recorded data will be time stamped. Few data points, prior to triggering of recorder, has to be recorded to capture the power system disturbances at which thumper is triggered.

4.2.1 Measurement system connection diagram

The connection methodology of measurement, recording and signal transmission system is shown in Fig. 4.2 and Fig. 4.3.

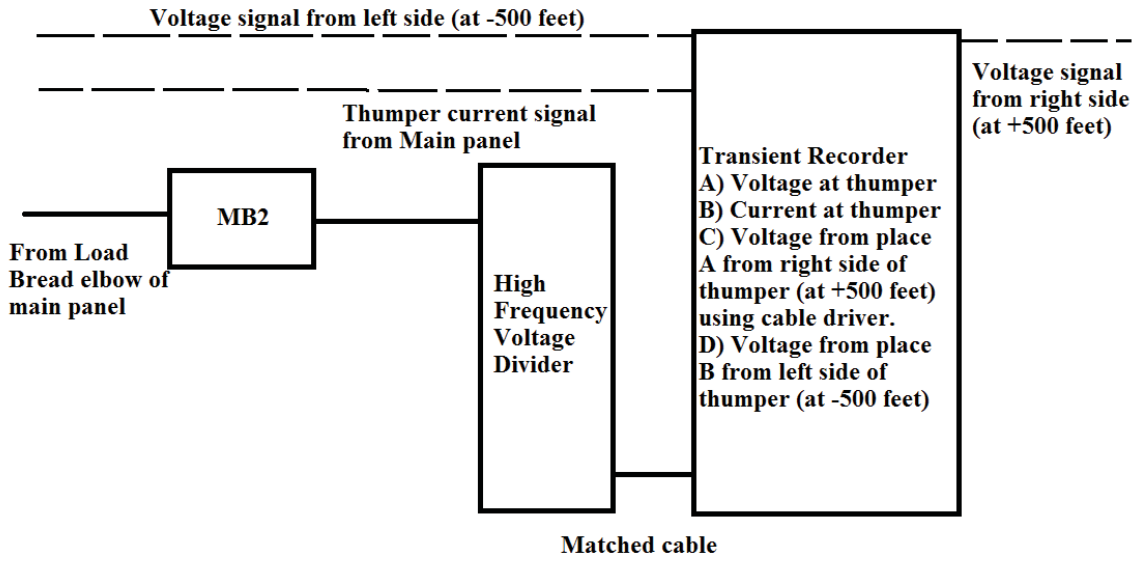

Figure 4.2 Measurement and Recorder panel component details (at thumper end)

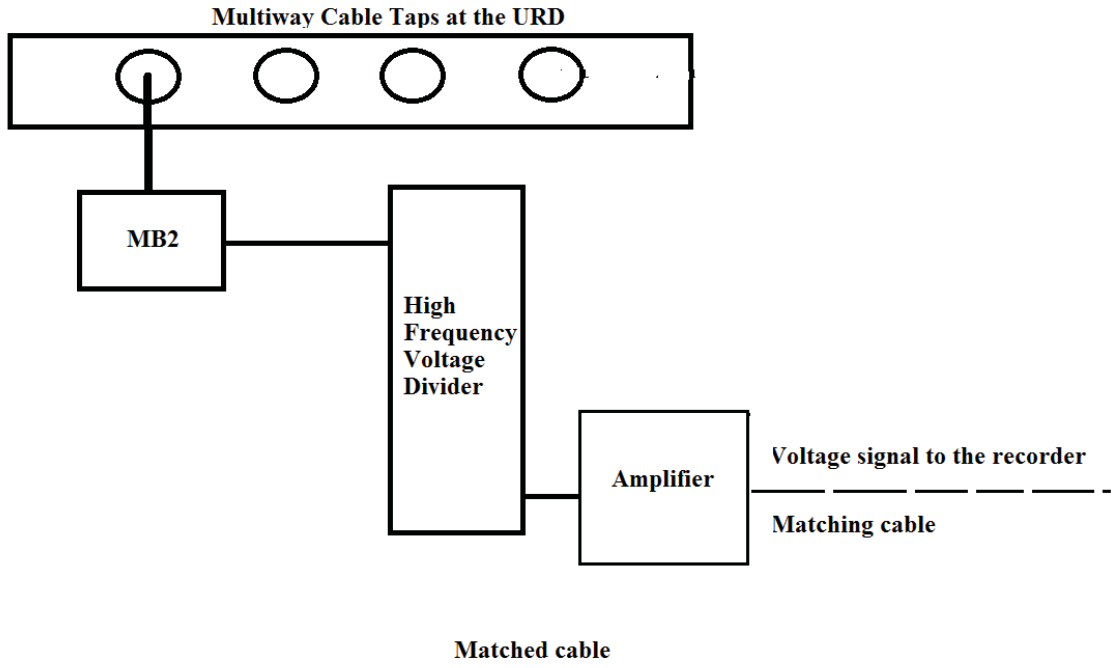

Figure 4.3 Measurement and Transmitting panel component details

4.2.2 Current Measurement

- Thumper current measurement is located in the main panel. Based on analysis, peak current magnitude may rise up to 2000A momentary in

thumper. A wideband (High Frequency) CT which is capable of measuring current up to 5 MHz and peak current of 2000 A was selected for installation.

4.2.3 Voltage Measurement

- Voltage divider is to be installed in recorder panel. Based on analysis, peak voltage magnitude will rise up to 15-20 kV momentarily. The values specified in [12] have similar ranges. A Wideband (High Frequency) voltage divider which is capable of measuring voltage up to 20 kV and has bandwidth up to 5 MHz is selected.
- Because of the nature of differential measurements, a pair of matched voltage dividers which are capable of measuring up to 5 MHz of applied voltage were selected.
- A main circuit breaker (MB2) for safety purpose is selected to be placed in recording panel, which can also be controlled manual/remote.
- Matching cables are used to connect voltage divider to transient recorder. Measurements from either end of the cable are to be done with similar setup. Matched signal amplifiers will be used to amplify and transmit the signals from divider to the recorder every 152.4 meter. Twisted pair cable with good screening should be preferred to transmit signal from one end to another [5].

4.2.4 Recording issues and mitigation

- The measurements recorded in the transient recorder will shift in time due to propagation delay of the signals in the cable. By knowing the

characteristics of the signal cable, this effect will be taken care in signal processing.

- Triggering and recording of different channels of the transient recorder can be independent. The effects of signal propagation delay will be completely mitigated if the recorder saves the transients triggered by individual dv/dt signal.
- Signal cables (152.4 meter long) of same length is to be used to transmit the signal from either end of thumper to recorder. This will mitigate the problem of time delay associated with differential measurements.

4.2.5 Noise issues and mitigation: Grounding

- Common ground point will be implemented by solid grounding of all the equipments and recording instruments to a single ground point in URD.
- Voltage measurement from other end of the cables will contain more noise, which cannot be avoided through grounding techniques.
- Equipments need to have a proper electromagnetic shielding for 0-2 MHz. Metal faraday cage will also be used for additional electromagnetic sielding [8].

4.2.6 Noise issues and mitigation: Calibration and noise level identification

- Several sets of system voltages and thumper currents at various angles of power frequencies will be recorded prior to trigger thumper. A similar set of system voltages and thumper current will be recorded after triggering thumper.

- The stored set of power frequency voltages and thumper current will contain valuable information about noise in the system. Signal processing tool should be used to identify the noise level based on the stored data [24]. The proper signal processing tools which will be required for calibration of noise will be identified based on the measurements of the pilot project.

4.2.7 Reflections and Attenuation issues

- Analysis reveals that 2 MHz signals are getting attenuated below -3 dBV (30% attenuation) at 182.88 meter from source.
- Until 152.4 meter of measurement, the attenuation is within -3 dBV for all frequencies of our interest. For 304.8 meter away from the source, the attenuation will be within -3 dBV for frequencies up to 0.5 MHz.
- The reflected wave also gets damped and when it reaches the sources, it has travelled twice the distance and is damped more than 30%. There are also partial reflections and attenuations introduced in the measurements from the joints and every cable taps, hence, adding more complexities in measurements beyond 152.4 meter to determine the state of cable insulation. Hence measurements are to be made every 152.4 meter on either side of the source.

CHAPTER V

CONCLUSION

The idea behind this work is to identify a measurement system to create intentional transients in URD system and to measure the transient along the length of the cable. To have better understanding of the characteristics of the transients, simulations of 12 kV Underground Residential Distribution system model in EMTP-RV were conducted. First the model was simulated and the results were verified with the test results provided by SDG&E. The model was simulated without power frequency to observe the transients along the URD. Next the model was simulated with power frequency on it and different thumper capacitance values. This simulation were carried out in order to obtain the best thumper values which induce measurable transients and at the same time do not induce harmful transients which will propagate along the URD. The simulations were carried out for different phase angle triggering of thumper to evaluate the effect of the power frequency voltage on thumper connection. The simulations were also carried out for different loading conditions to evaluate the effect of the loading of the URD on measurements. By the analysis of the results of these simulations, characteristics of the transients were listed. Based on the characteristics, the requirements of a measurement system were identified. The results were analyzed for differential measurements, and quantization noise. Based on all the analysis, a measurement system connection methodology and test plan for a pilot project was devised.

5.1 Future work

In order to realize the ultimate goal of the work, a pilot project to build the measurement system and record the transients has to be setup. Measurement systems required for the test have to acquire and build as per the specifications developed from the work. Measurements have to be taken for good, degraded, and neutral corroded power cables. Based on the pilot project recorded transients, signal processing of recorded data and statistical analysis of recorded data could be carried out in order to develop an ageing and faulty cable insulation assessment model.

REFERENCES

[1] Thomas Owen Bialek, "Evaluation and Modelling of High-Voltage Cable Insulation using a High-Voltage Impulse", Ph.D. Dissetration. TK7 .B5354 2005, Mississippi State University, 2005.

[2] Toshikatsu Tanaka, Allan Greenwood, "Advanced Power Cable Technology – Volume I and Volume II", CRC Press, 1983.

[3] Andrew R. Hileman, "Insulation Coordination for Power Systems", Marcel Dekker, Inc, 1999.

[4] David M. Pozar, "Microwave Engineering", 2nd Ed., John Wiley & Sons, Inc, 1998.

[5] R.E. Martin, "Electrical Interference in Electronic Systems : Its Avoidance within High-Voltage Substations and Elsewhere", Research Studies Press, 1979.

[6] A. Setayeshmehr, H. Borosi, E. Gockenbach, I. Fofana, "On-line Monitoring of Transformer via Transfer Function," 2009 IEEE Electrical Insulation Conference, Montreal, QC, Canada, pp. 278-282, 31 May – 3 June, 2009.

[7] P. Werelius, P. Tharning, R. Eriksson, B. Holmgren, U. Gafvert, "Dielectric Spectroscopy for Diagnosis of Water Tree Deterioration in XLPE Cables", IEEE Transactions on Dielectrics and Electrical Insulation, Vol. 8, No1, pp. 27-42, February 2001.

[8] IEEE 1122 – 1998, "IEEE Standard for Digital Recorders for Measurements in High- Voltage Impulse Tests", 1998.

[9] Michael Cerna, Audrey F. Harvey, "The Fundamentals of FFT-Based Signal Analysis and Measurement", Application Note 041, National Instruments, 2000.

[10] T. Tsujimoto I, M. Nakade I, Y. Yagi K. Adachi, H. Tanaka, "Development of on-site diagnostic method for XLPE cable by harmonics in AC Loss Current", Proceedings of the 7th International Conference on Properties and Applications of Dielectic Materials, June 1-5, 2003, nagoya, Japan.

[11] C. M. Wiggins, D. E. Thomas, T. M. Salas, F. S. Nickel, H. W. Ng, "A NOVEL CONCEPT FOR URD CABLE FAULT LOCATION", IEEE Transactions on Power Delivery, Vol 9, No. 1, January 1994.

[12] N. Kolcio, J.A.Halladay, G.D.Allen, E.N.Fromholtz, "Transient Overvoltages and Overcurrents on 12.47 kV Distribution Lines: Field Test Results", IEEE Transactions on Power Delivery, Vol. 7, No.3, July 1992.

[13] R.A.Walling, R.D.Melchior, B.A.McDermott, "Measurement of Cable Switching Trnasients in Underground Distribution Systems", IEEE Transactions on Power Delivery, Vol. 10, No. 1, January 1995.

[14] L. Marti, "Simulation of Transients in Underground Cables with Frequency-Dependent Modal Transformation Matrices",IEEE Transaction on Power Delivery, Volume 3, No. 3, July 1988.

[15] T. Nakayama, "On-Line Cable Monitor Developed in Japan",IEEE Transaction on Power Delivery, Volume 6, No. 4, October 1991.

[16] A. Nakajima, N. Kashiwagi, T. Murata, S. Takahashi, 0. Fukuda, S. Kitai, K. Tokumaru, K. Hirotsu, "Development of a Hot-line Diagnostic Method for XLPE Cables and the Measurement Results",IEEE Transaction on Power Delivery, Volume 4, No. 2, July 1989.

[17] S . Grzybowski, R.L. McMellon, "Electrical Breakdown Strength of XLPE Cables under Combined AC-DC Voltage", IEEE Southeastcon 1995, Visualize the Future, North Raleigh Hilton Raleigh, NC, pp. 63 to pp. 66, March 1995.

[18] B.H. Ward, J.P. Steiner, "An Alternative to DC Testing of Installed Polymeric Power Cables", 7th International Symposium on High Voltage Engineering, Dresden, Germany, August 26-30, 1991, pg. 177-180.

[19] E. Gulski et al, "PD Diagnosis and Condition Assessment of Distribution Power Cables using Damped AC Voltages", XIII International Symposium on Voltage Engineering, Netherlands 2003.

[20] T.O. Bialek and S. Grzybowski, "Investigation of the Performance of New XLPE and EPR Cables", IEEE 1999 Conference on Electrical Insulation and Dielectric Phenomena , Oct. 17-20, 1999, Austin, Texas.

[21] T.O. Bialek, S. Grzybowski, "Investigation of the Performance of Field Aged HMWPE and XLPE Cables", IEEE 2000 Conference on Electrical Insulation and Dielectric Phenomena , Oct. 15-18, 2000, Victoria, British Columbia, Canada.

[22] L. Cao, A. Zanwar, B. Pushpanathan, S. Grzybowski, “Electrical Aging of 15 kV EPR Cable Energized by AC Voltage with Switching Impulses Superimposed”, 2010 International Conference on High Voltage Engineering and Application, Oct. 11-14, 2010, New Orleans, Lousiana, USA.

[23] T. Leibfried and K. Feser, “On-Line Monitoring of Transformers by Means of the Transfer Function Method”, IEEE International Symposium on Electrical Insulation, Pittsburgh, Pennsylvania, June 1994, pg 111-114.

[24] Matthew S. Mashikian, Francesco Palmieri, Rajeev Bansal, Robert B. Northrop, “Location of Partial Discharges in Shielded Cables in the Presence of High Noise”, IEEE Transaction on Electrical Insulation, Vol. 27, No. 1, February 1992, pg. 37 - 43.

[25] B. Holmgren et al, “Correlation Between AC Breakdown Strength and Low Frequency Dielectric Loss of Water Tree Aged XLPE Cables”, IEEE Transactions on Power Delivery, Vol. 13, No. 1, January 1998, pg. 40-45.

[26] J. Densley, “Ageing Mechanisms and Diagnostics for Power Cables – An Overview”, IEEE Electrical Insulation Magazine, Vol. 17, No. 1, January/February 2001, pg. 14-22.

[27] R. Reid, “High Voltage VLF Test Equipment With Sinusoidal Waveform”, IEEE Transactions on Power Delivery, Vol. 12, No. 2, April 1997, pg. 565-570.

[28] Y. Akutsu et al, “Insulation Deterioration Monitoring System for Ungrounded Power Distribution Systems”, IEEE/PES 1993 Summer Meeting, Vancouver, Canada, July 1993, SM 406-9 PWRD.

[29] M. Aihara et al, “Application of GPT to Tanδ Measuring Apparatus for Distribution Cable in Hot Line”, IEEE/PES 1991 Winter Meeting, New York, New York, February 1991, 91 WM 251-9 PWRD

[30] M. Kosaki et al, “New Approach to Diagnostic Method of Water Trees”, IEEE International Symposium on Electrical Insulation, Toronto, Canada, June 3-6, 1990, pg. 296-299.

[31] G.S. Eager Jr. et al, “Effect of DC Testing Water Tree Deteriorated Cable and a Preliminary Evalution of VLF as Alternative”, IEEE Transactions on Power Delivery, Vol. 7, No. 3, 1992, pg. 1582-1591.

[32] C.J. Doman and S.J. Heyer, “AC Testing Without Cable Degradation”, Transmission and Distribution World, July 1999.

[33] V. Buchholz and S. Cherukupalli, “Review of Emerging Cable Test Methods for Condition Assessment of Underground Distribution Cable Assets”, 1999 IEEE PES T&D Conference, New Orleans, Louisiana, April 1999, Panel Session #9.

[34] P. Werelius, “Power Cable Diagnostics by Dielectric Spectroscopy”, 1999 IEEE PES T&D Conference, New Orleans, Louisiana, April 1999, Panel Session on Diagnostic Measurement Techniques For Power Cables.

[35] E. Gockenbach and W. Hauschild, “The Selection of the Frequency Range for High-Voltage On-Site Testing of Extruded Insulation Cable Systems”, IEEE Electrical Insulation Magazine, Vol. 16, No. 6, November/December 2000, pg. 11-16.

[36] P. Tharning and P. Werelius, “High Voltage Dielectric Response Analyzer for Cable Diagnostics”, IEEE Conference on Electrical Insulation and Dielectric Phenomena, Pocono Manor, Pennsylvania, October 1993, pg. 745-750.

[37] E. Hanique, “A Transfer Function is a Reliable Tool for Comparison of Full and Chopped Lightning Impulse Tests”, IEEE PES 1994 Winter Meeting, New York, New York, January 30 – February 4, 1994, 94 WM 149-5 PWRD.

[38] R. Malewski and B. Poulin, “Impulse Testing of Power Transformers Using the Transfer Function Method”, IEEE Transactions on Power Delivery, Vol. 3, No. 2, April 1988, pg. 476-489.

[39] T. Leibfried and K. Feser, “Some Aspects using the Transfer Function Concept in High Voltage Impulse Testing of Transformers”, International Symposium on Digital Techniques in High-Voltage Measurements, Toronto, Canada, October 28-30, 1991, pg. 5.3-5.7.

[40] J. Douville et al, “Measurement of Switching Transients in 735 kV Substations and Assessment of Their Severity for Transformer Insulation”, IEEE Transactions on Power Delivery, Vol. PWRD-3, No. 4, 1989, pg. 1380-1387.

APPENDIX A

CABLE MODEL SIMULATION AND VALIDATION

A.1 Response of 1000 kcmil XLPE cable of 152.4 meter length, Non-energized, open-ended

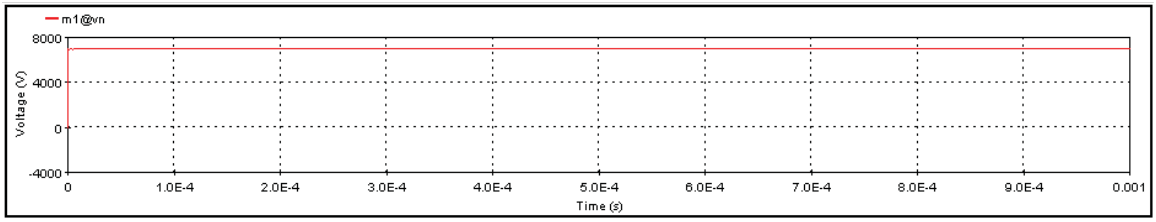

a) Voltge at Thumper, Point A

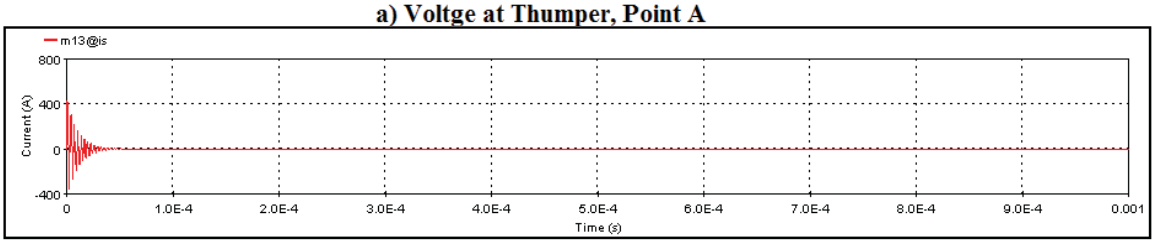

b) Current at Thumper, Point A

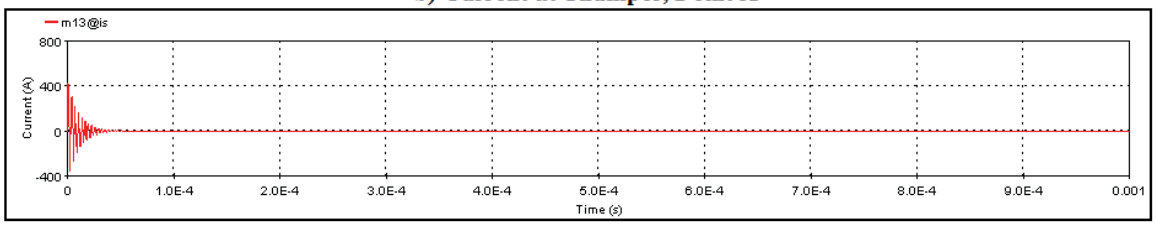

c) Voltage at 500ft, Point B

Figure A.1 Simulation result for 152.4 meter cable

A.2 Response of the cable of 762 meter non-energized, open-ended with branching cable of 91.44 meter open-ended

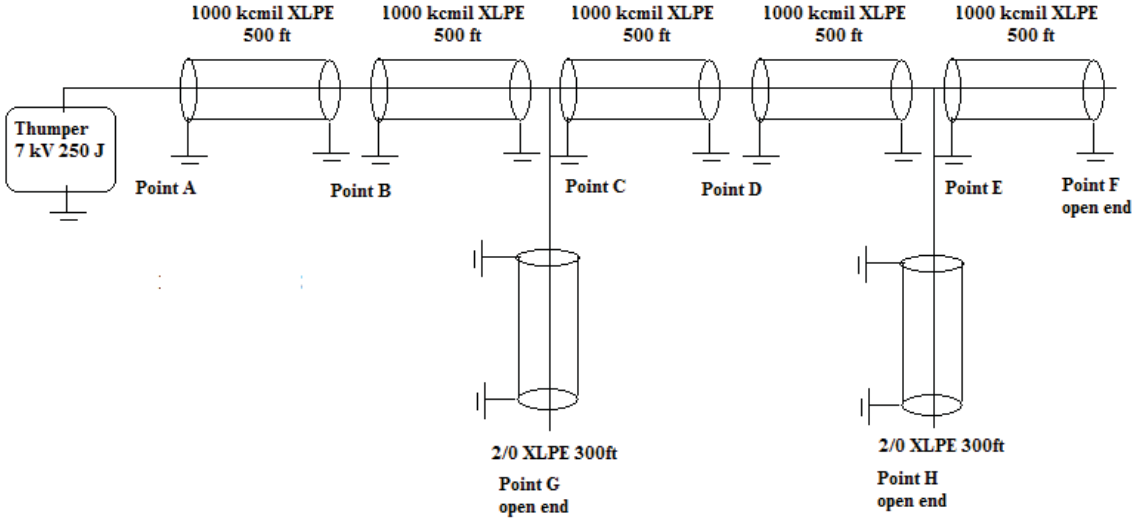

Figure A.2 762 meter (2500 feet) non-energized unloaded URD model

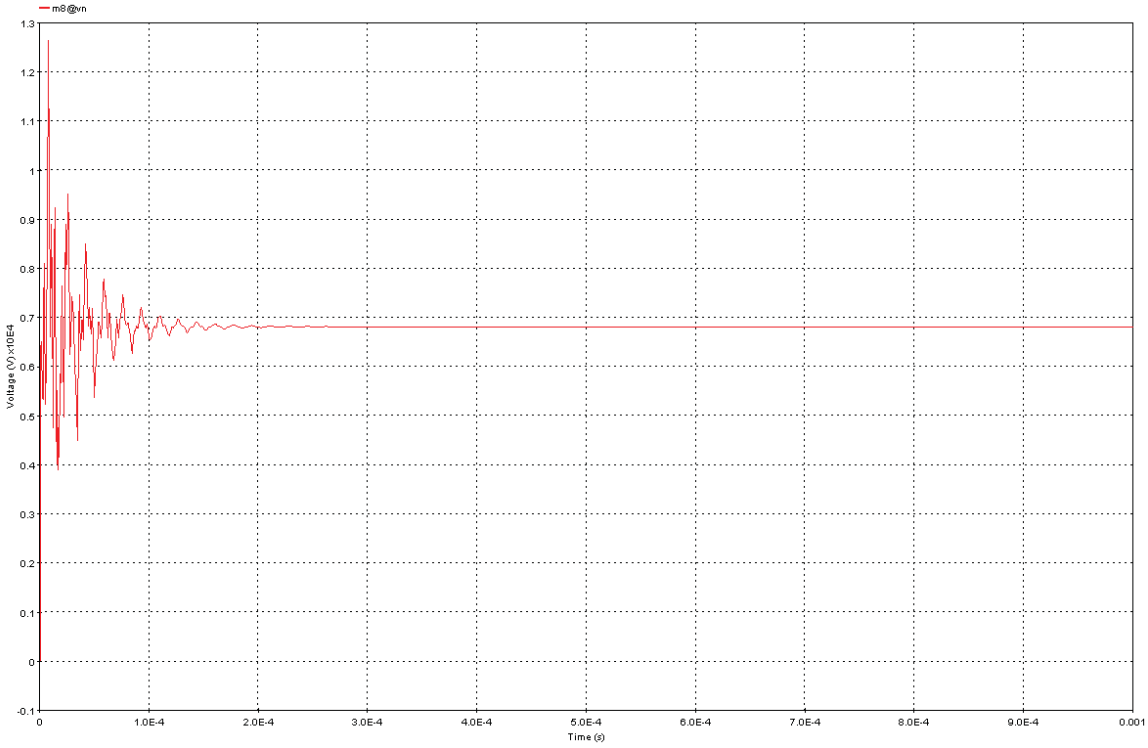

Figure A.3 Voltage at 152.4 meter, Point B

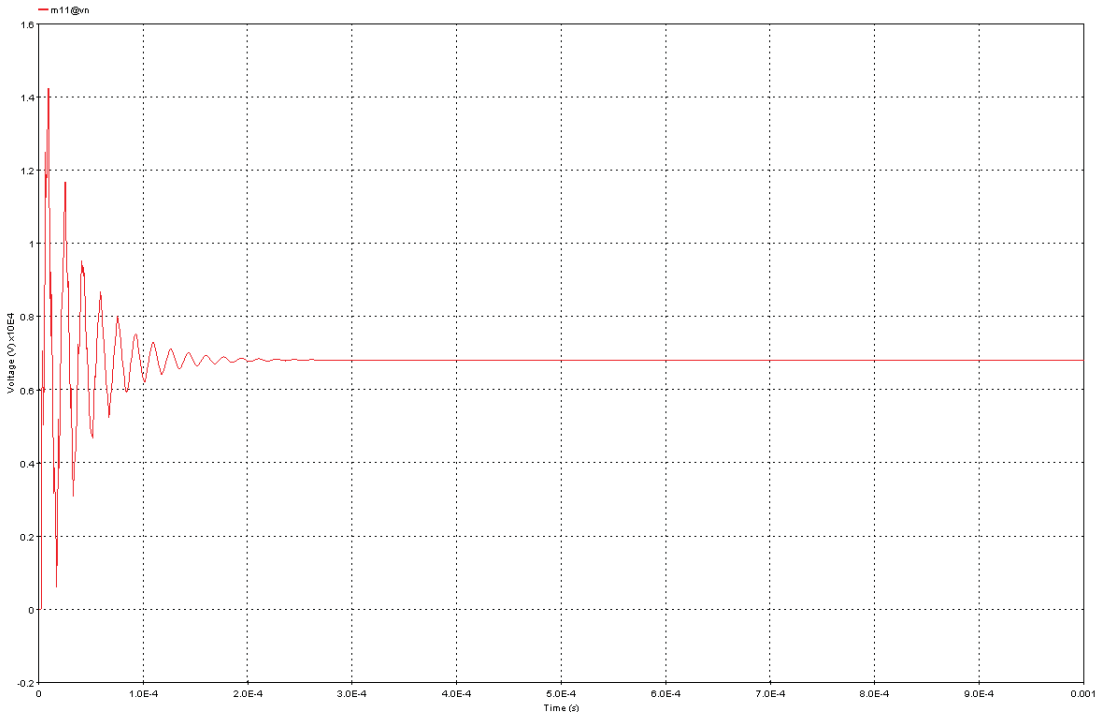

Figure A.4 Voltage at 457.2 meter, Point D

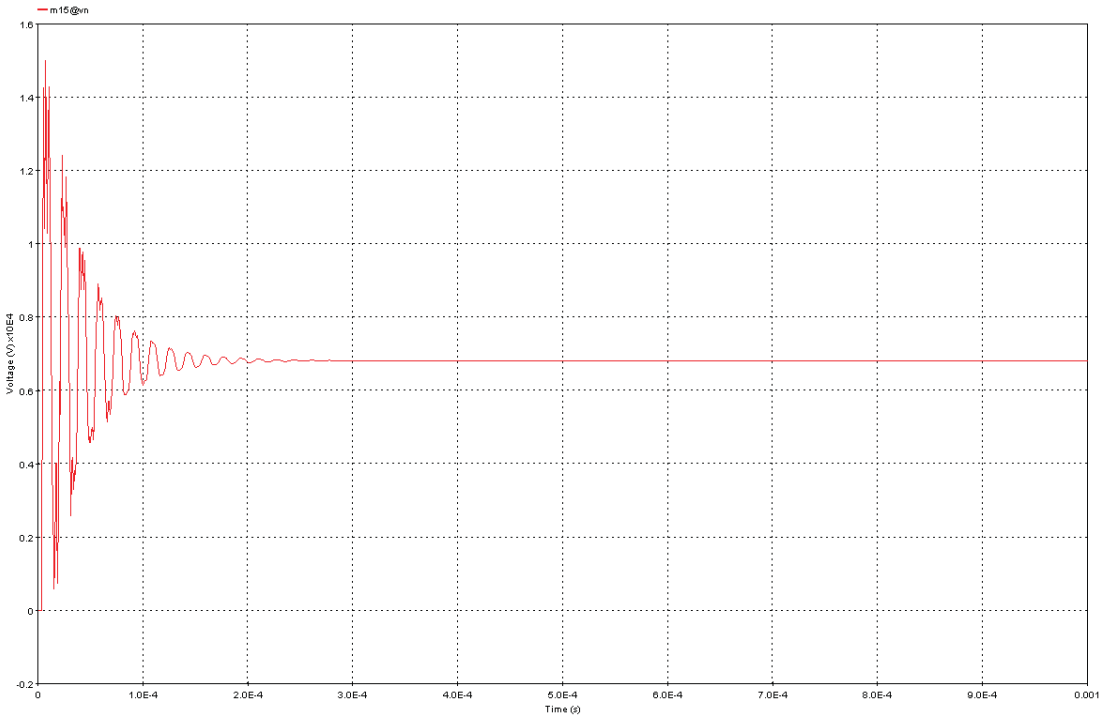

Figure A.5 Voltage at 762 meter, Point F

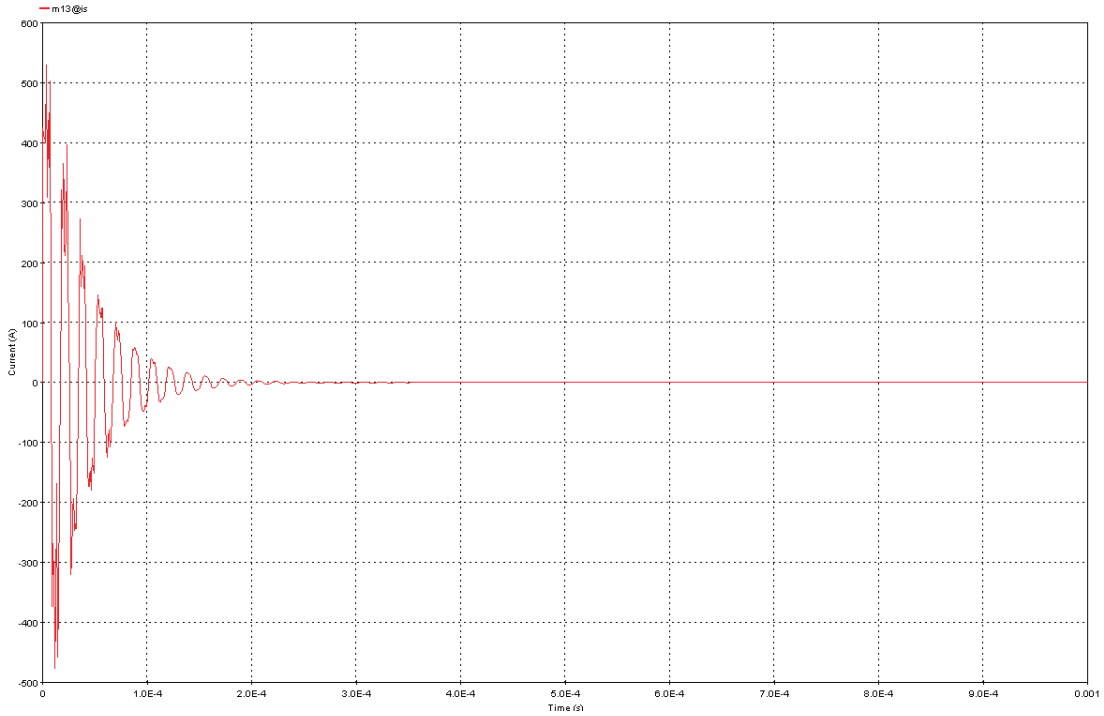

Figure A.6 Current at thumper

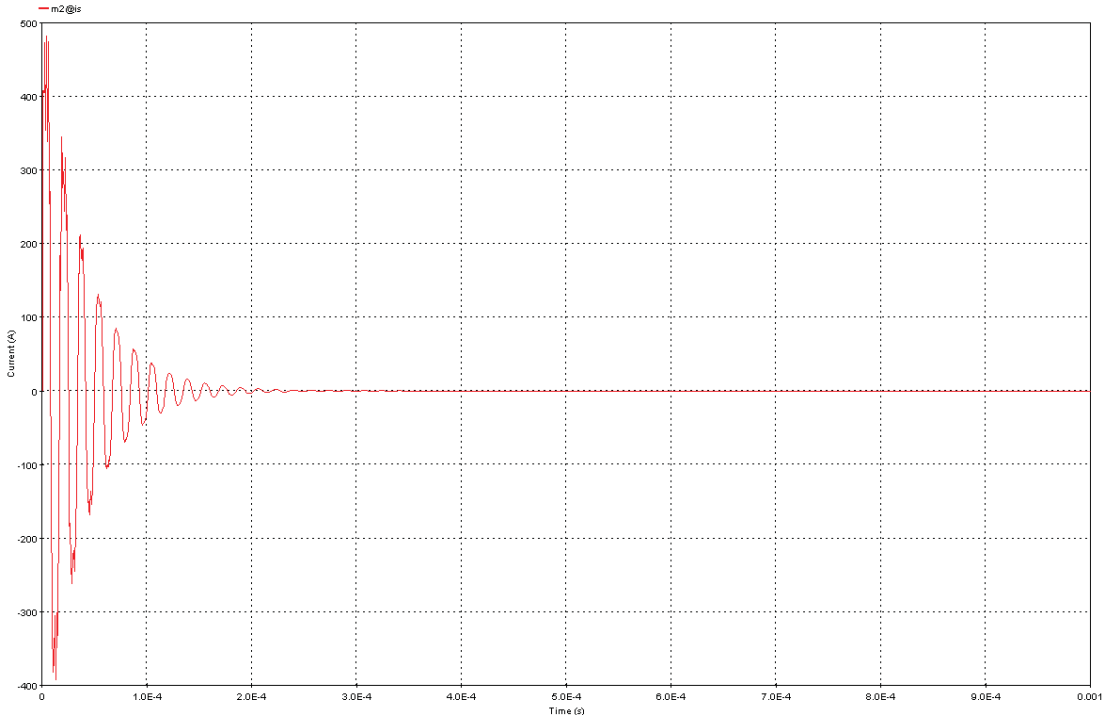

Figure A.7 Current at 152.4 meter

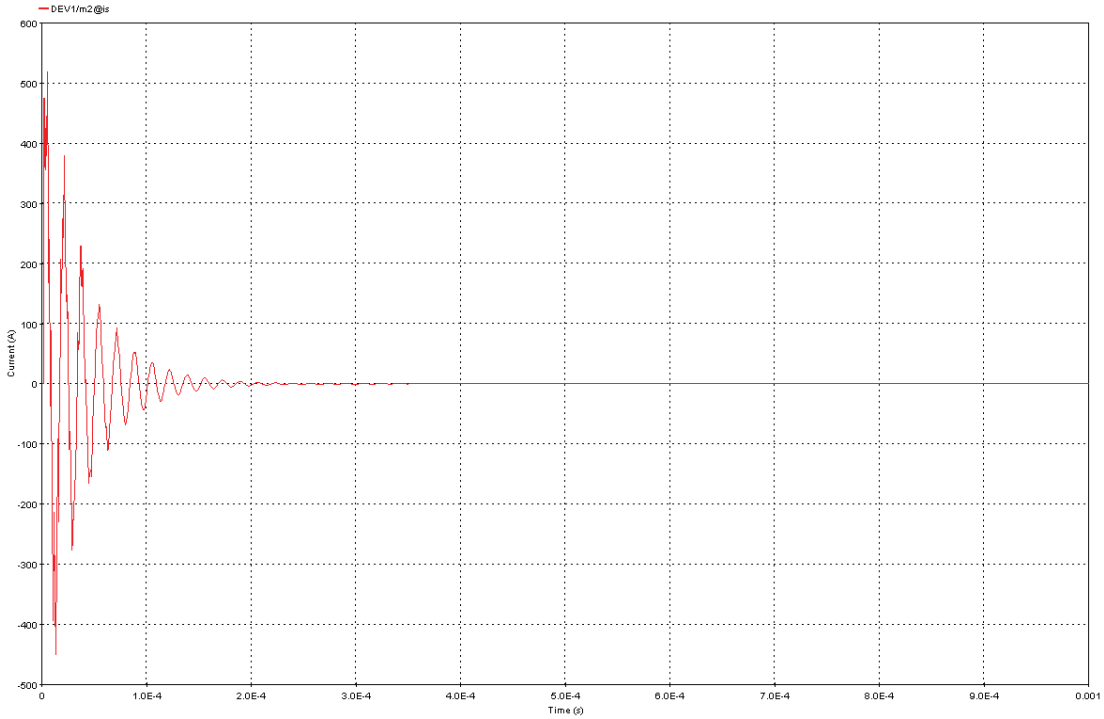

Figure A.8 Current at 304.8 meter

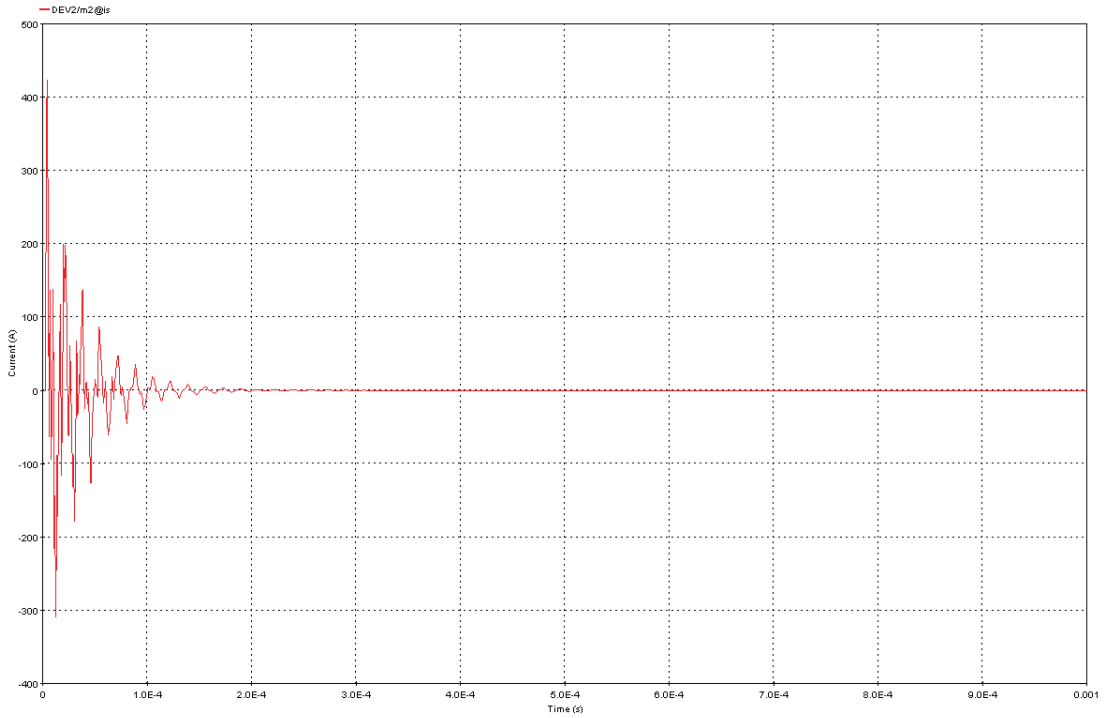

Figure A.9 Current at 457.2 meter

APPENDIX B

NON-ENERGIZED UNDERGROUND RESIDENTIAL DISTRIBUTION SYSTEM MODEL SIMULATION AND ANALYSIS

B.1 Voltage and Current waveform at different points in the model as function of time, time domain results. (762 meter URD)

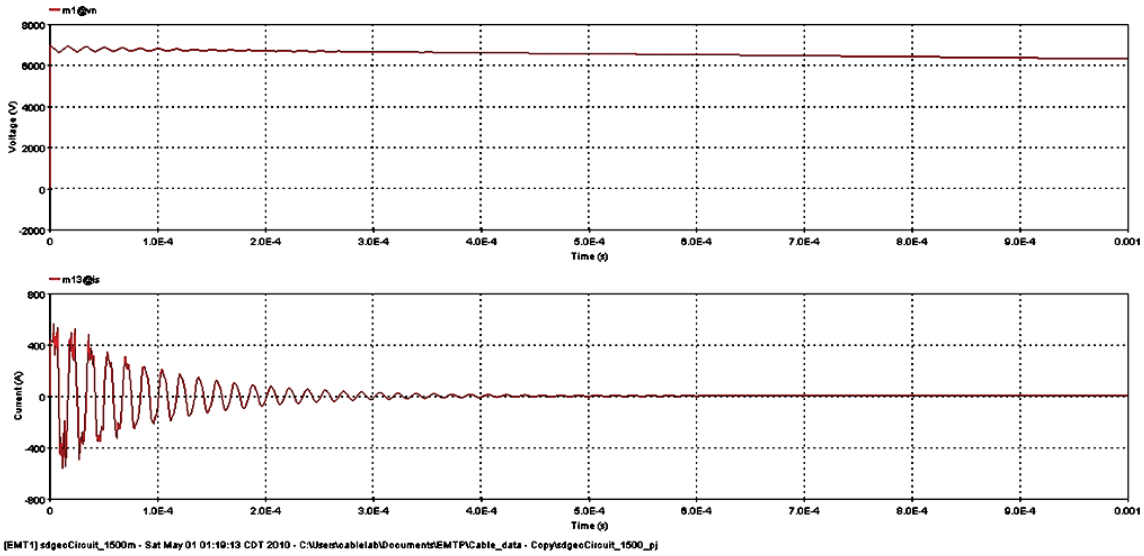

Figure B.1 Voltage and Current at Thumper function time, Point A

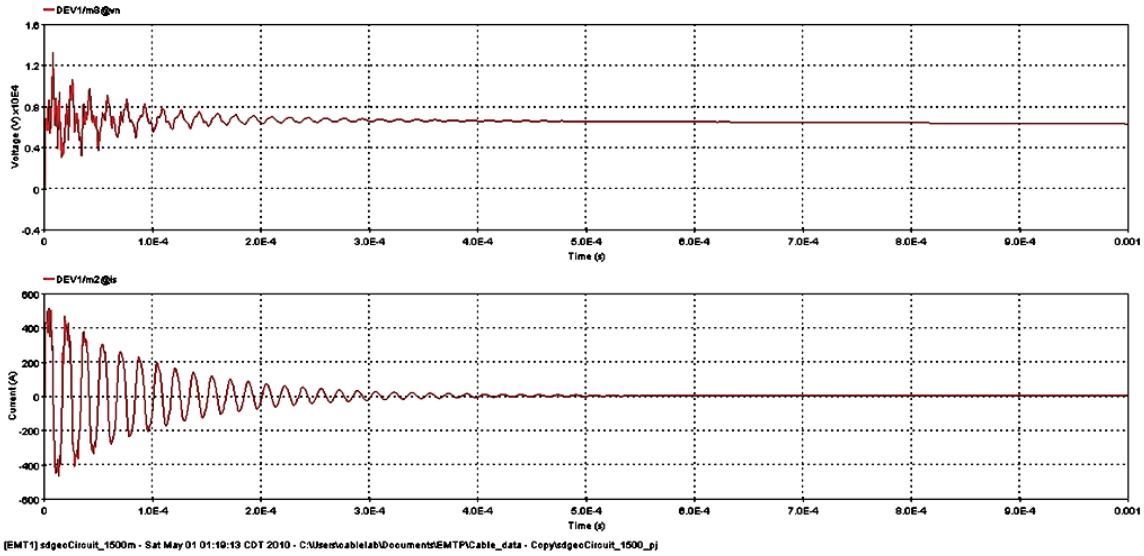

Figure B.2 Voltage and Current at 152.4 meter from Thumper function time, Point B

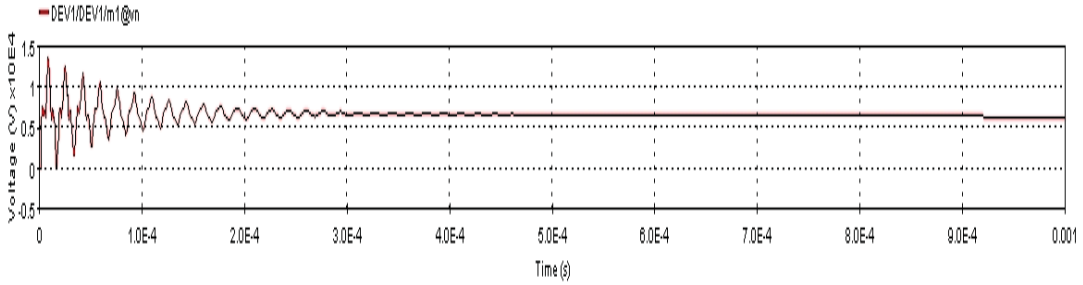

Figure B.3 Voltage function at 304.8 meter from Thumper, Point C.

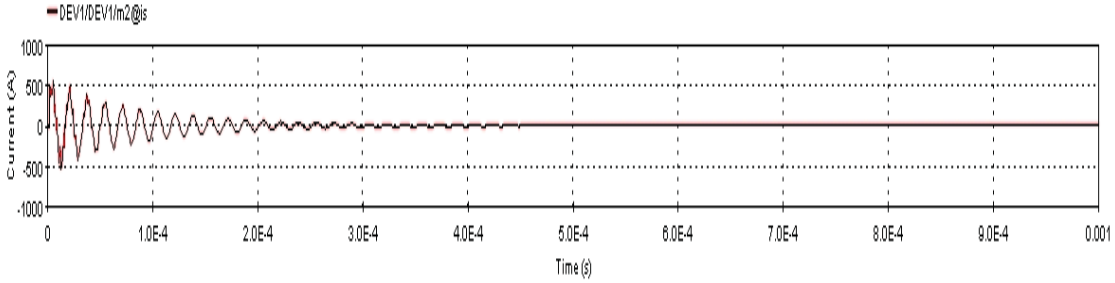

Figure B.4 Current function time at 304.8 meter from Thumper on incoming cable, Point C.

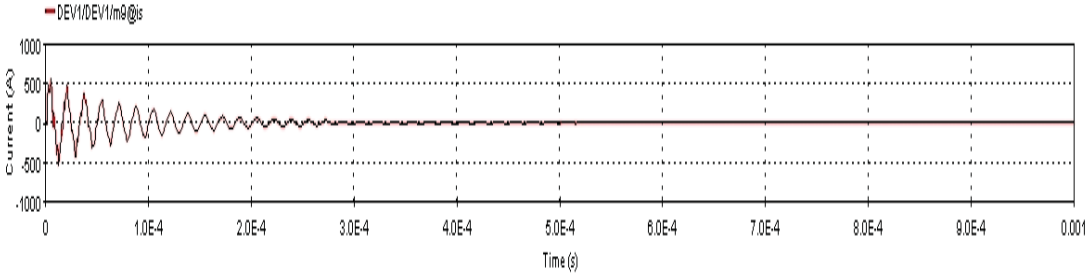

Figure B.5 Current function time at 304.8 meter from Thumper on outgoing cable, Point C.

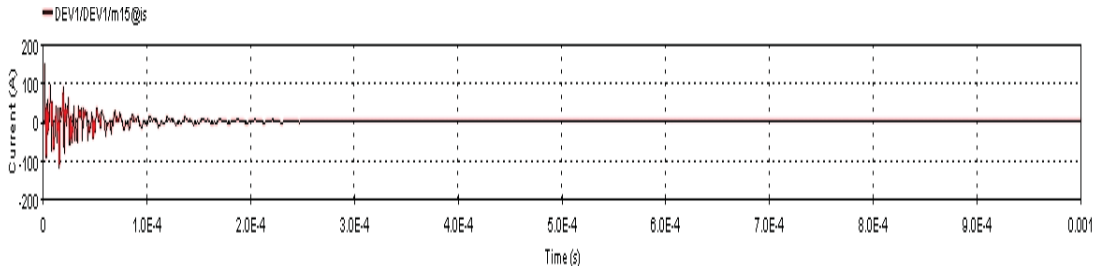

Figure B.6 Current function time at 304.8 meter from Thumper on radial cable, Point C.

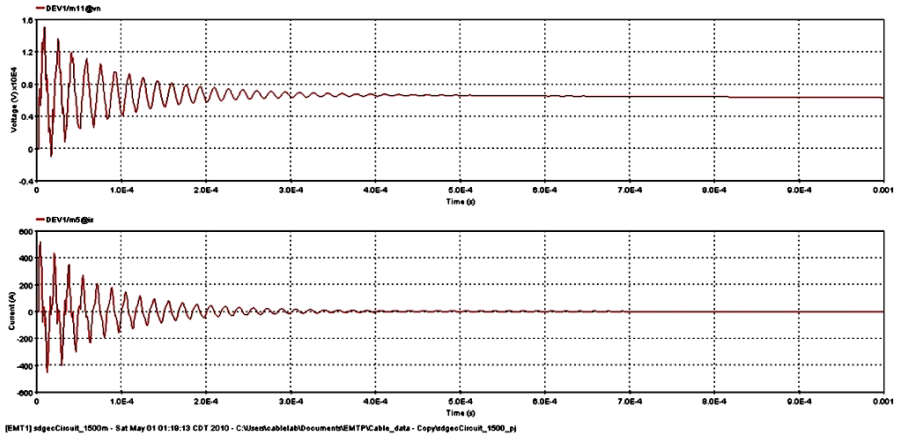

Figure B.7 Voltage and Current function time at 457.2 meter from Thumper, Point D.

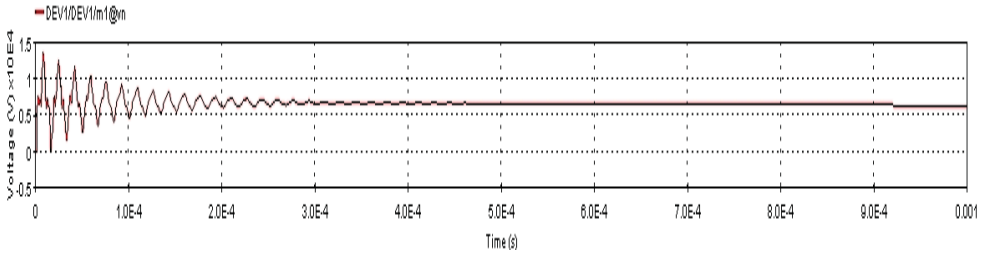

Figure B.8 Voltage function time at 609.6 meter from Thumper, Point E.

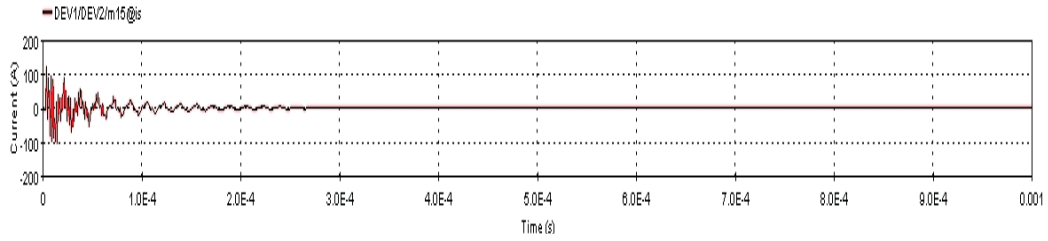

Figure B.9 Current function time at 609.6 meter from Thumper on incoming cable, Point E

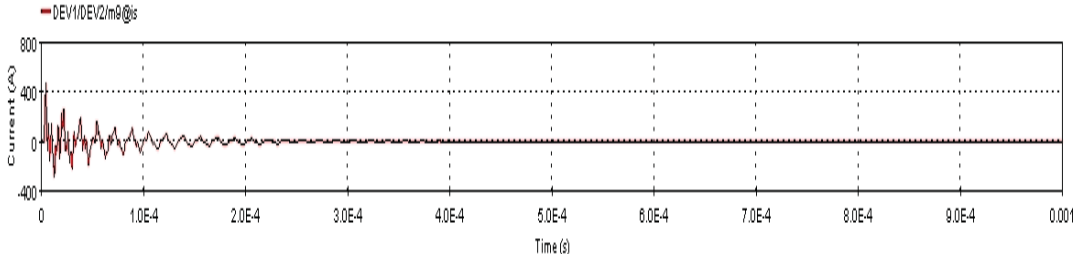

Figure B.10 Current function time at 609.6 meter from Thumper on outgoing cable, Point E

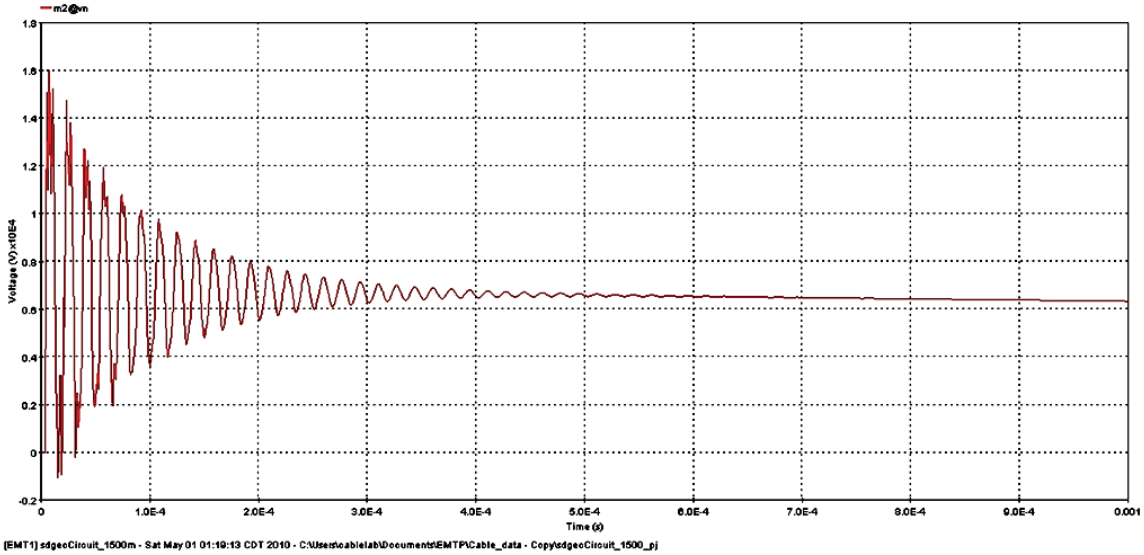

Figure B.11 Voltage function time at 762 meter from Thumper, Point F

B.2 Frequency content of Voltage and Current waveform, single-sided frequency spectrum at different points in the model as function of time, time domain results. (762 meter URD)

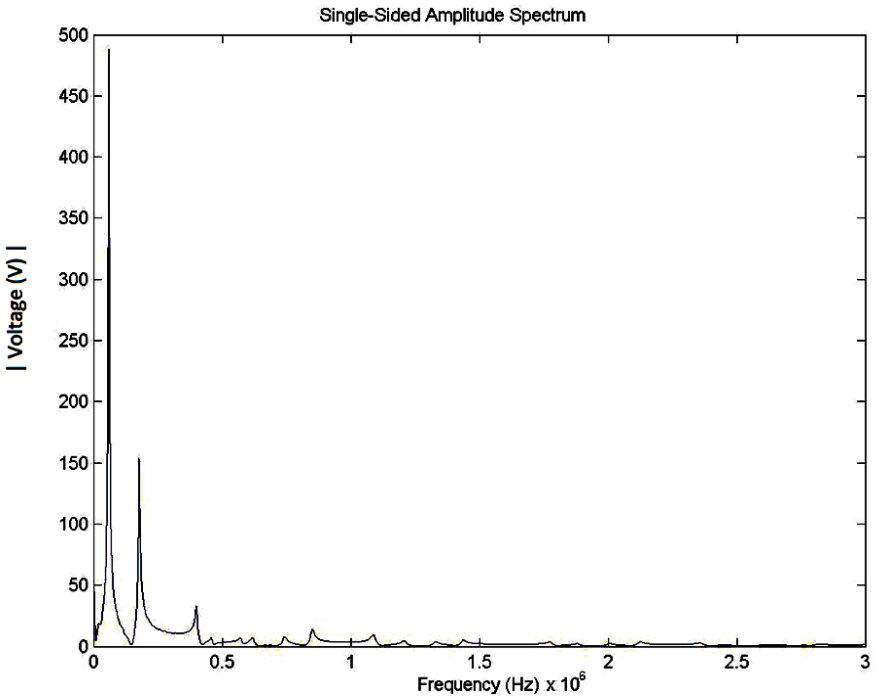

Figure B.12 Frequency spectrum of voltage at 304.8 meter from Thumper, Point C

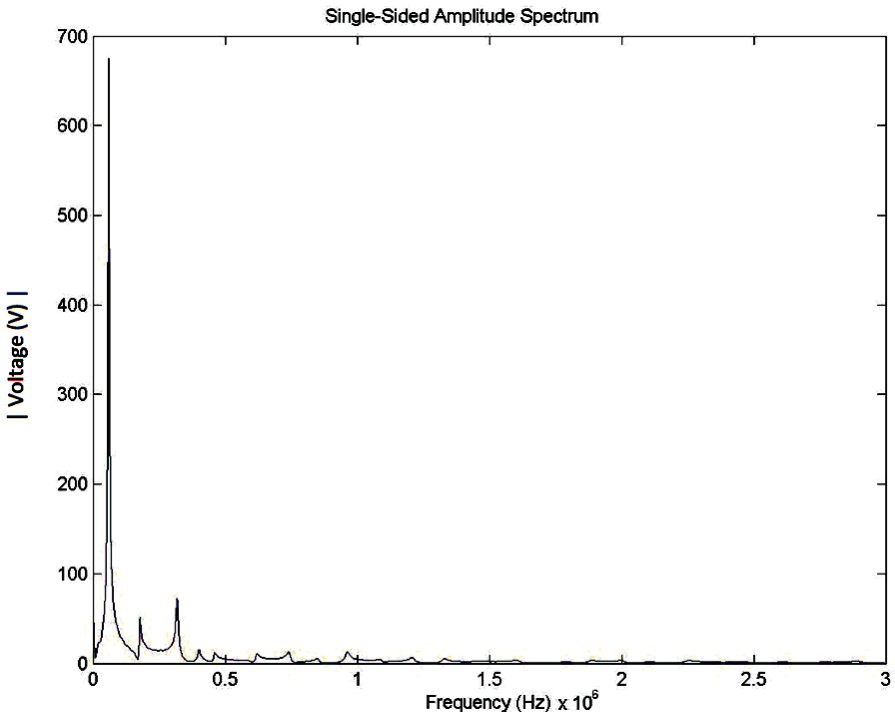

Figure B.13 Frequency spectrum of voltage at 457.2 meter from Thumper, Point D

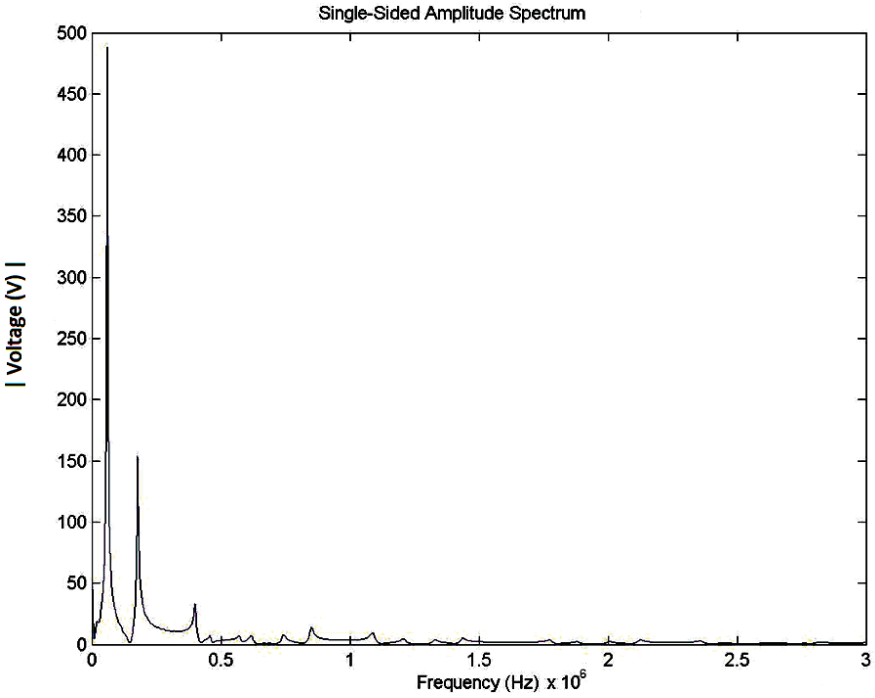

Figure B.14 Frequency spectrum of voltage at 609.6 meter from Thumper, Point E

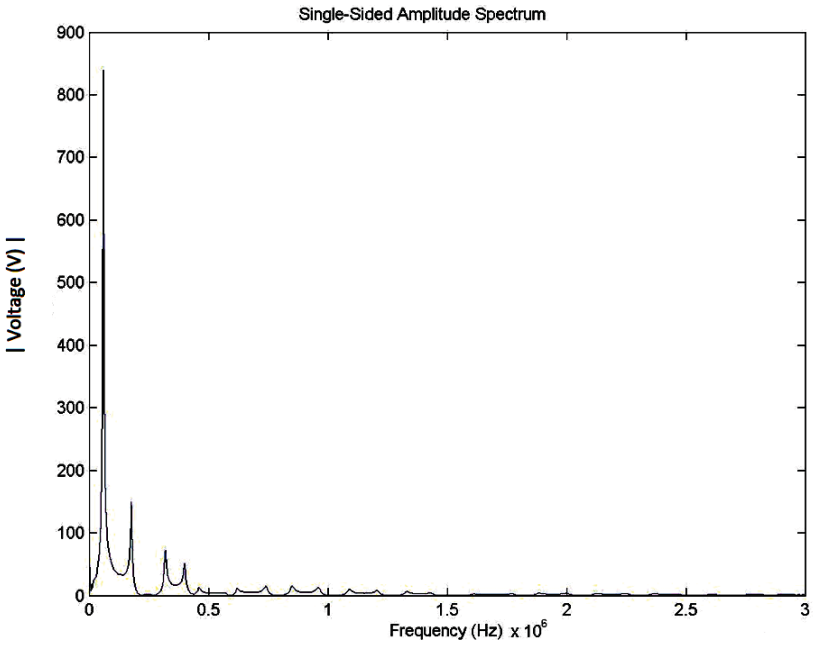

Figure B.15 Frequency spectrum of voltage at 762 meter from Thumper, Point F

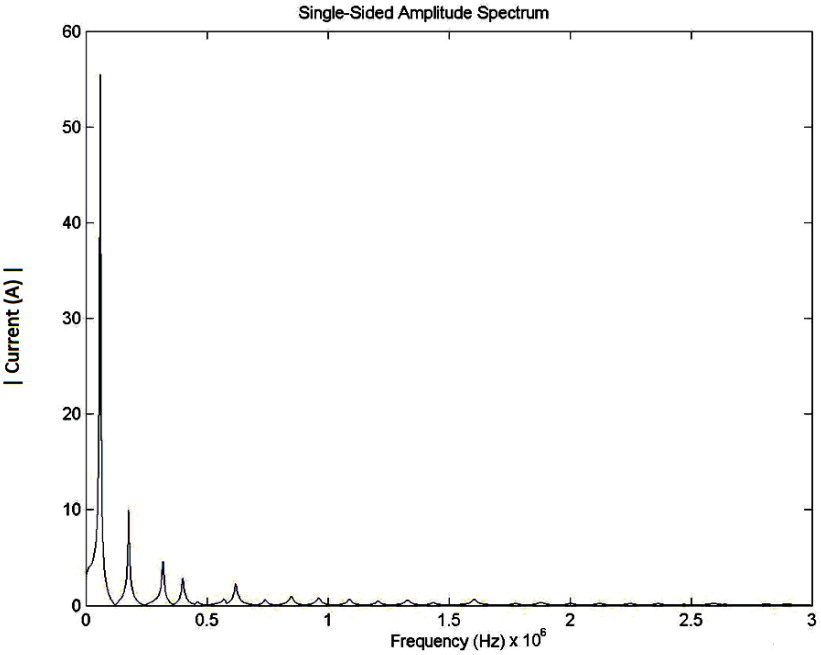

Figure B.16 Frequency spectrum of current at Thumper, Point A

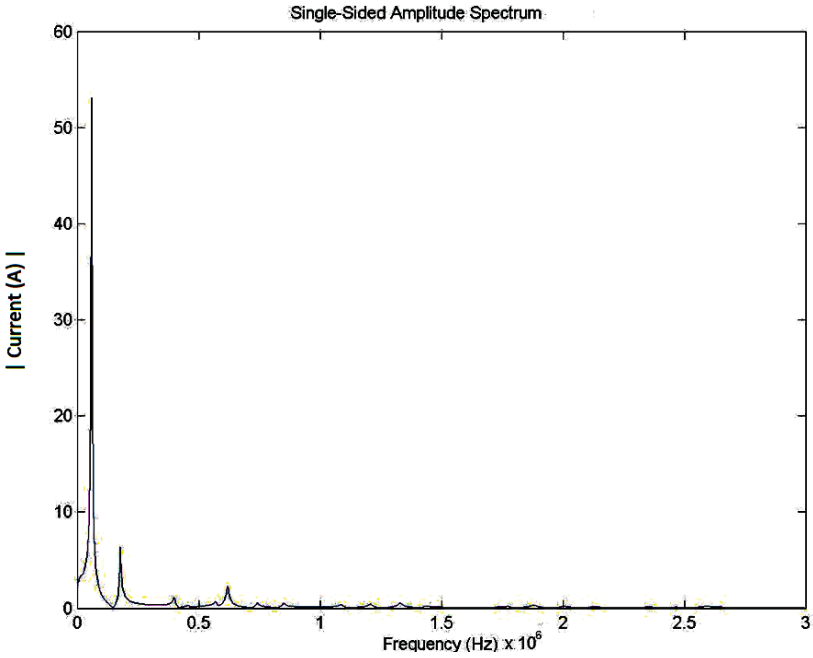

Figure B.17 Frequency spectrum of current at 152.4 meter from Thumper, Point B

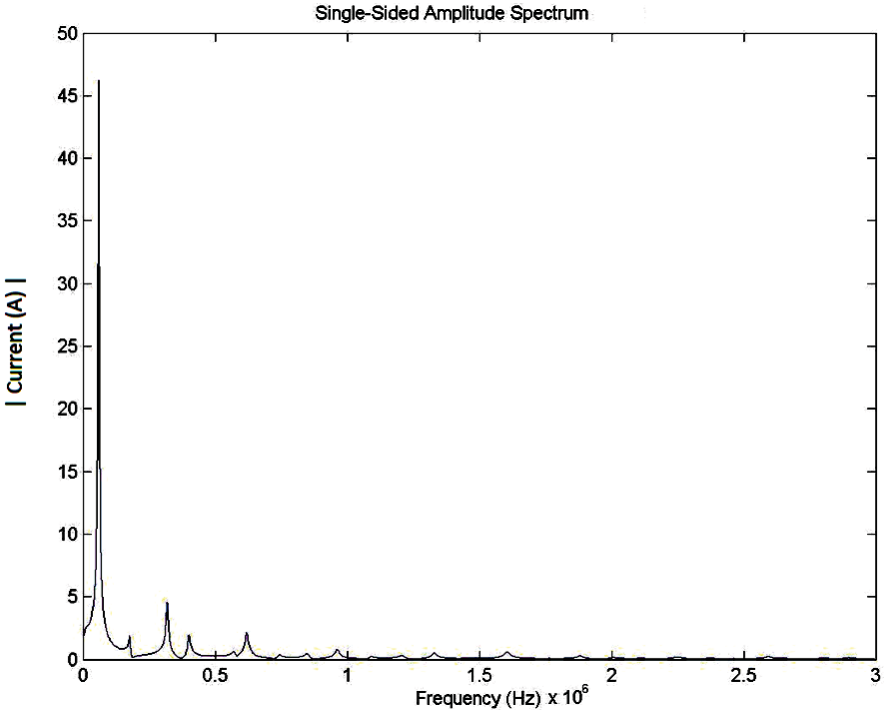

Figure B.18 Frequency spectrum of current at 304.8 meter from Thumper, incoming cable, Point C

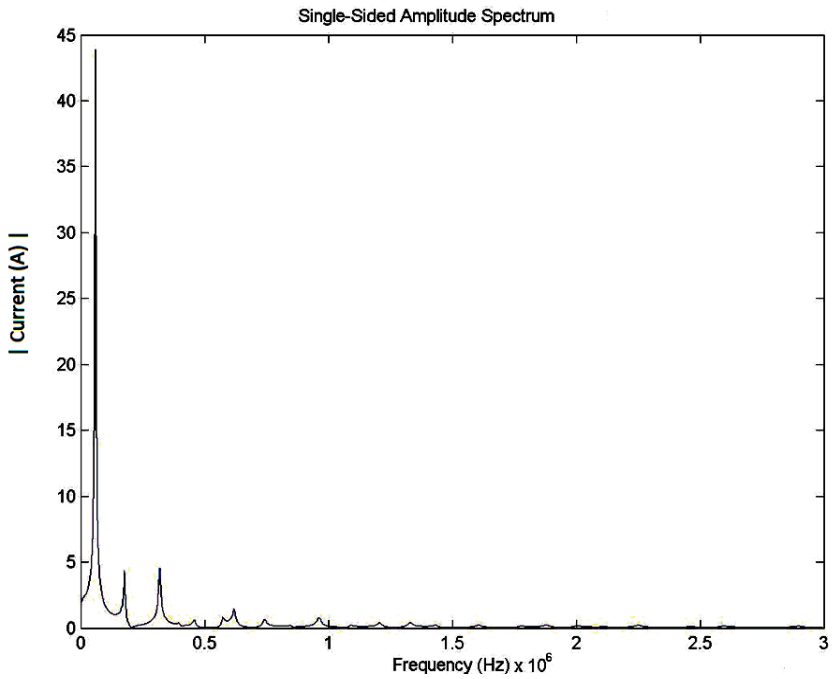

Figure B.19 Frequency spectrum of current at 304.8 meter from Thumper, outgoing cable, Point C

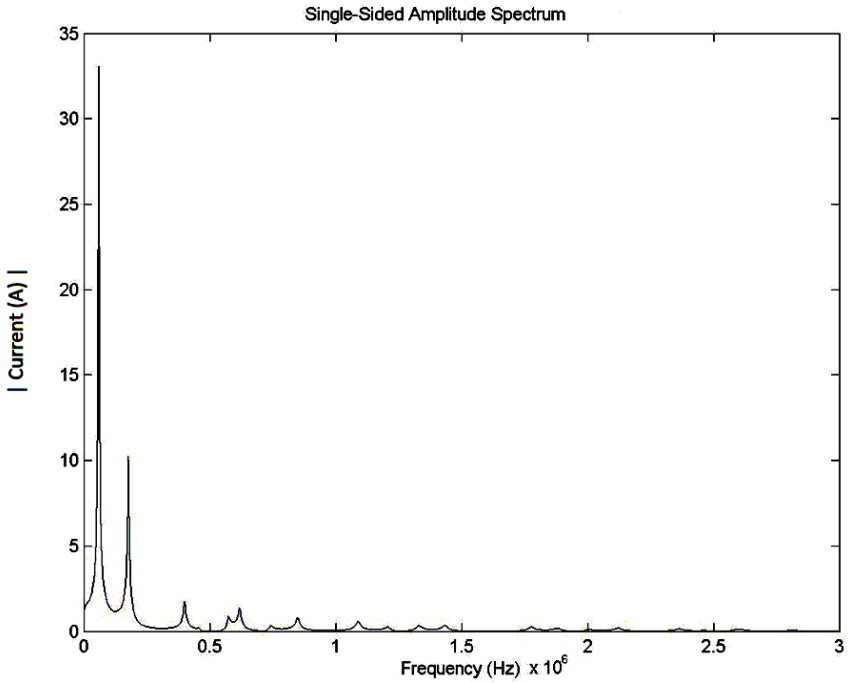

Figure B.20 Frequency spectrum of current at 457.2 meter from Thumper, Point D

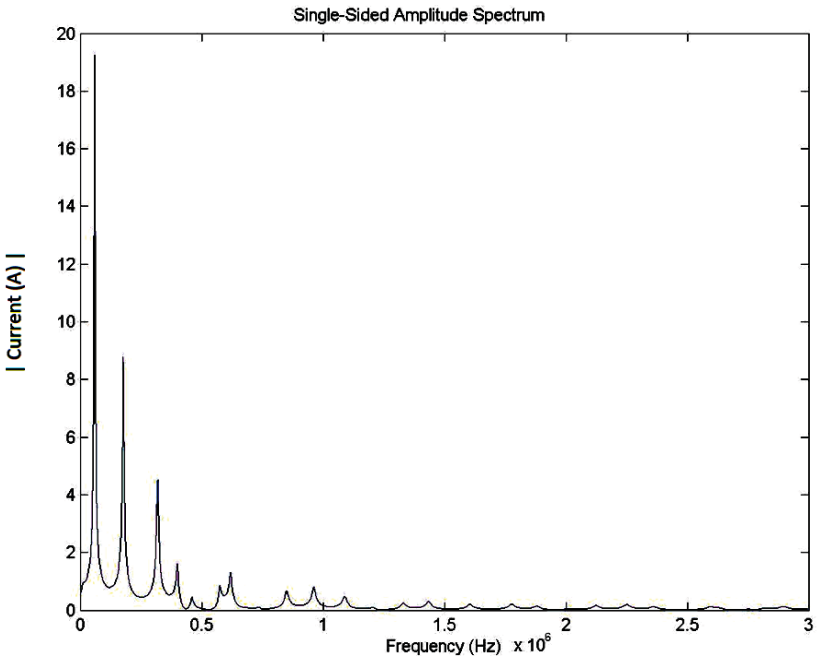

Figure B.21 Frequency spectrum of current at 609.6 meter from Thumper, incoming cable, Point E

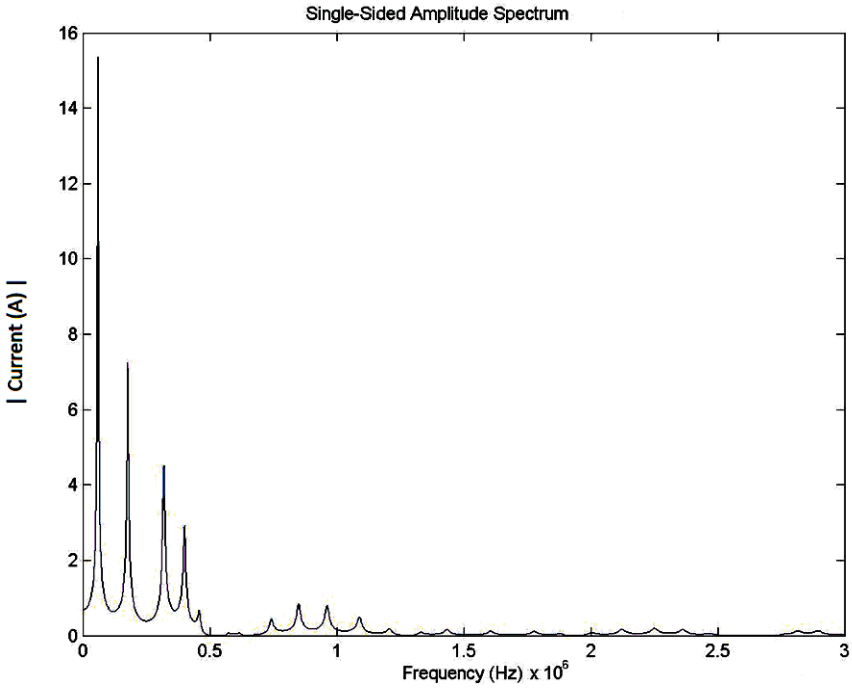

Figure B.22 Frequency spectrum of current at 609.6 meter from Thumper, outgoing cable, Point E

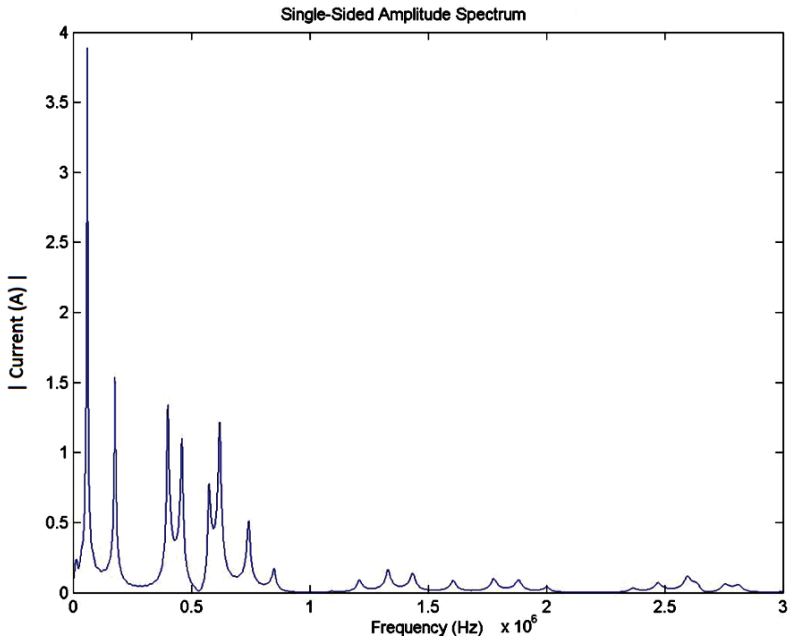

Figure B.23 Frequency spectrum of current at 609.6 meter from Thumper, radial cable to transformer, Point E

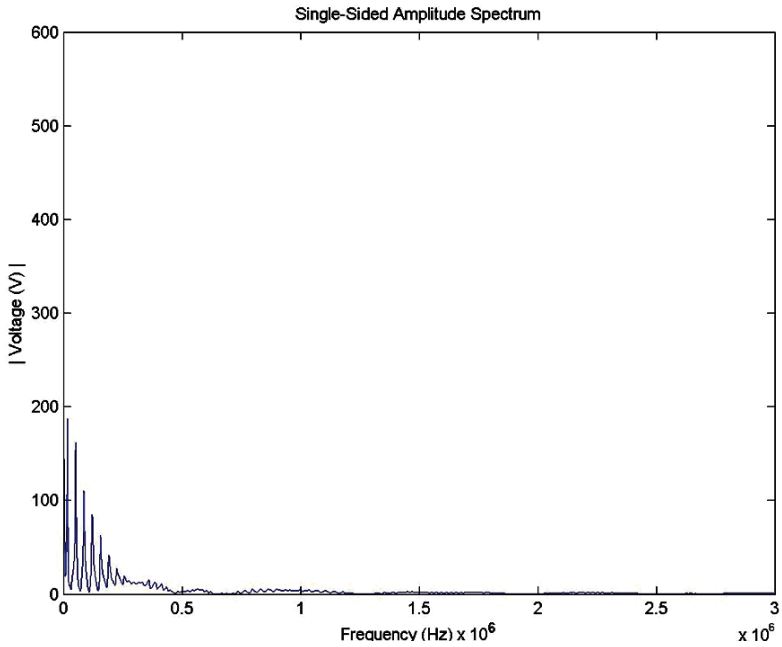

Figure B.24 Frequency spectrum of Voltage at 304.8 meter from Thumper, Point C of 2590.8 meter URD cable system

.

APPENDIX C

ENERGIZED UNDERGROUND RESIDENTIAL DISTRIBUTION SYSTEM MODEL SIMULATION AND ANALYSIS

C.1 Simulation of the energized URD for different phase angle trigger connection of thumper.

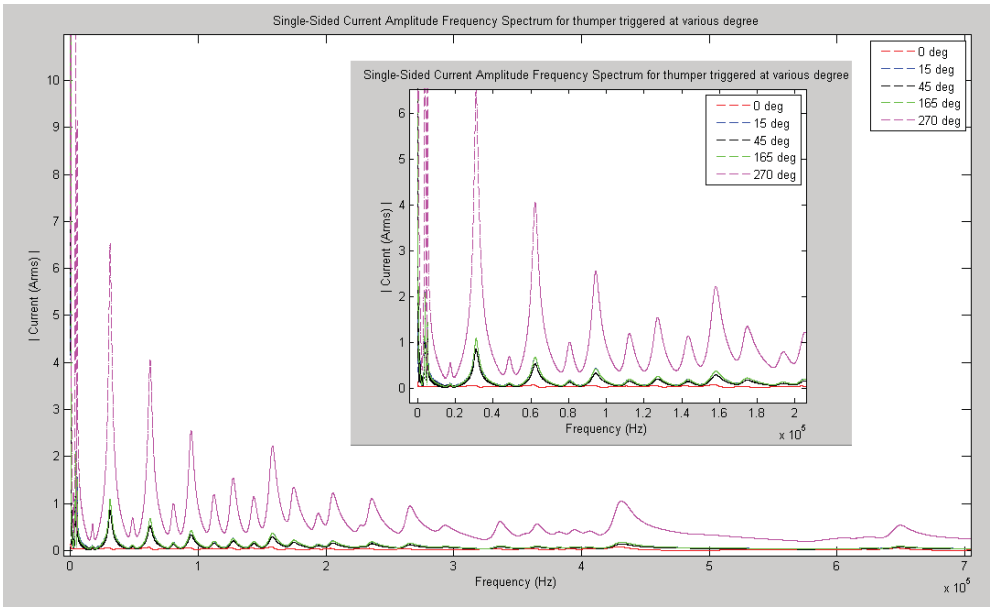

Figure C.1 Single-Sided Current Amplitude Frequency Spectrum for Thumper, triggered at various phase degree of power frequency

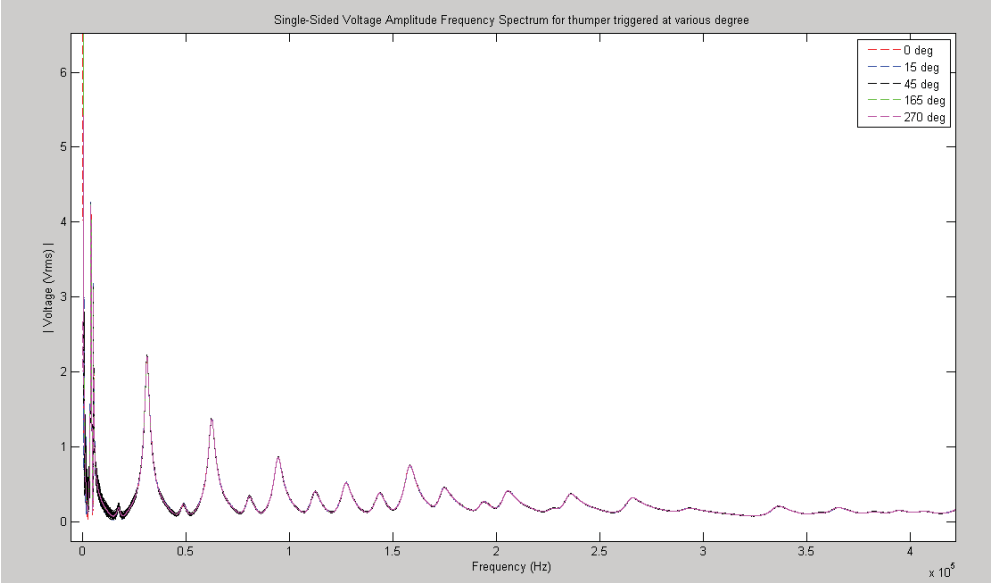

Figure C.2 Single-Sided Voltage Amplitude Frequency Spectrum for Thumper, triggered at various phase degree of power frequency, scaled by the ratio of difference between thumper voltage and power frequency instantaneous voltage

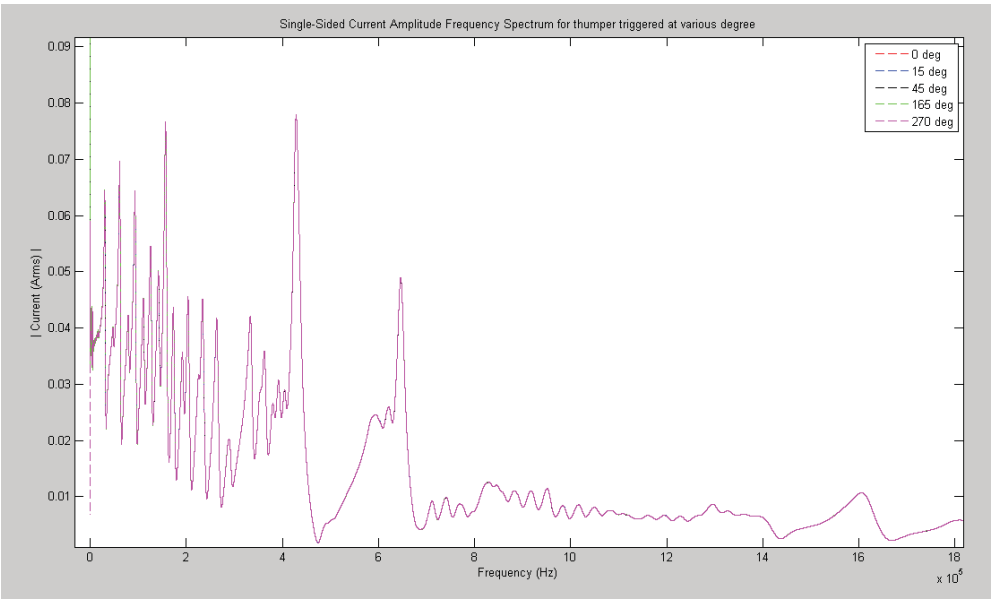

Figure C.3 Single-Sided Current Amplitude Frequency Spectrum for Thumper, triggered at various phase degree of power frequency, scaled by the ratio of difference between thumper voltage and power frequency instantaneous voltage

C.2 Simulation of the energized URD for thumper connected at different positions of the URD

In simulation results, the transients exist for 5 ms. This gives the total transient time, which is needed to be captured by the recording instrument. From Fig. C.4 & C.5, the frequency spectrum exits untill 3 MHz. However, the magnitude of the current and voltage spectrum beyond 2 MHz displays negligible value. This specifies the minimum sampling rate required by the recording instrument of 4 - 6 M Samples/second as per nyquist criteria.

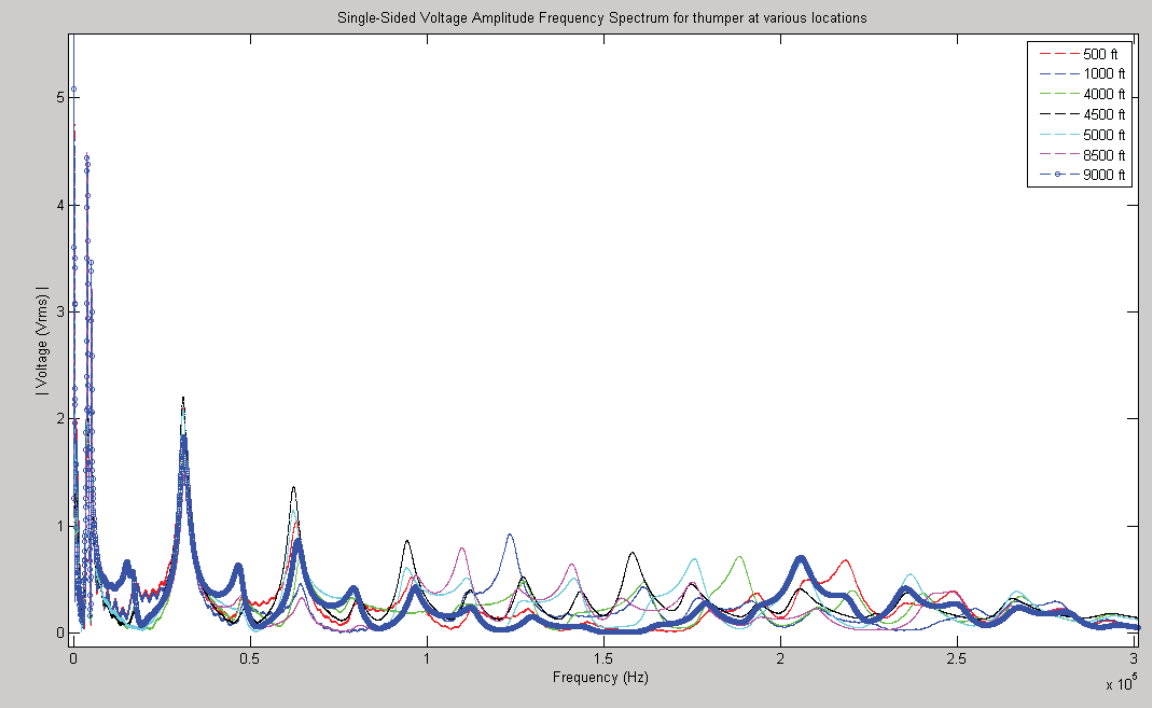

Figure C.4 Single-Sided Voltage Amplitude Frequency Spectrum for Thumper at Various Locations

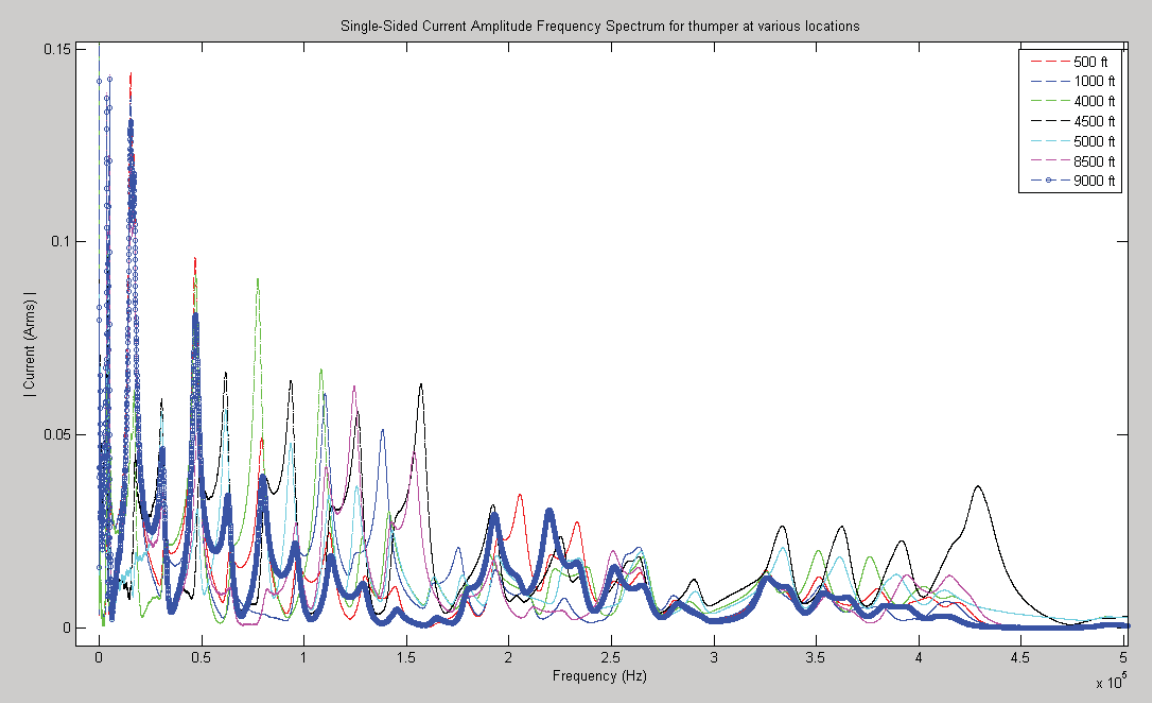

Figure C.5 Single-Sided Current Amplitude Frequency Spectrum for Thumper at Various Locations

C.3 Simulation of energized URD for differential measurements

Voltages were recorded at various places along the travel of the URD. They were recorded during the simulation of the energized URD for light loaded condition and when thumper was connected at Point J. The impulse travelled to other measurement positions of the cable. The analysis of recorded transients at various locations of cable for differential measurements could be performed by either non-synchronous voltage triggering or synchronous external triggering. From Fig. C.6 and Fig C.8, this effect of matching waveform until reflected wave from either end was seen in both synchronous and non-synchronous measurement.

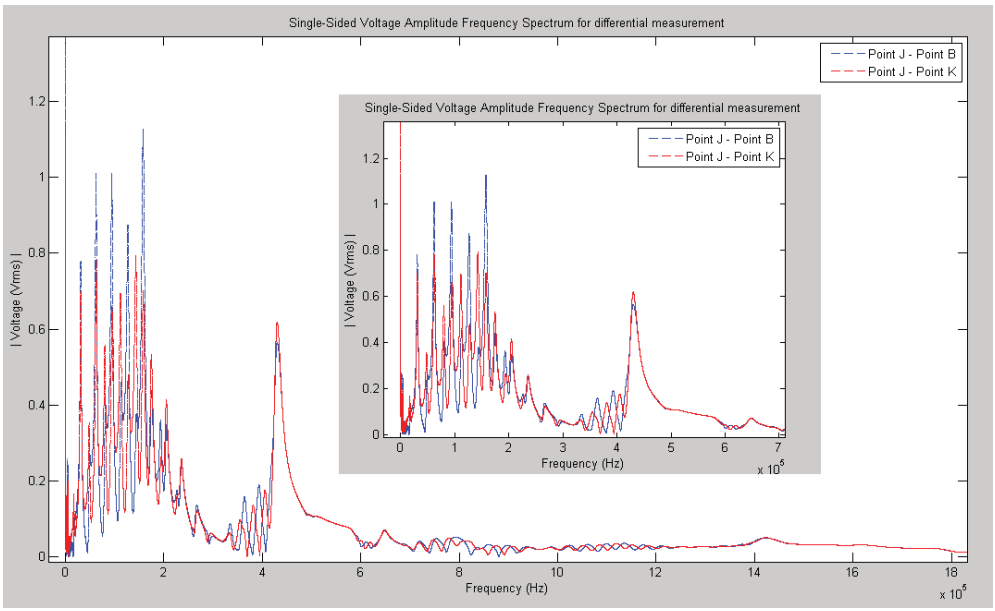

Figure C.6 Single-Sided Voltage Amplitude Frequency spectrum for Differential Measurement with the measurement on either side of thumper (Point B and Point K), shifted in time to represent non-synchronous differential measurement

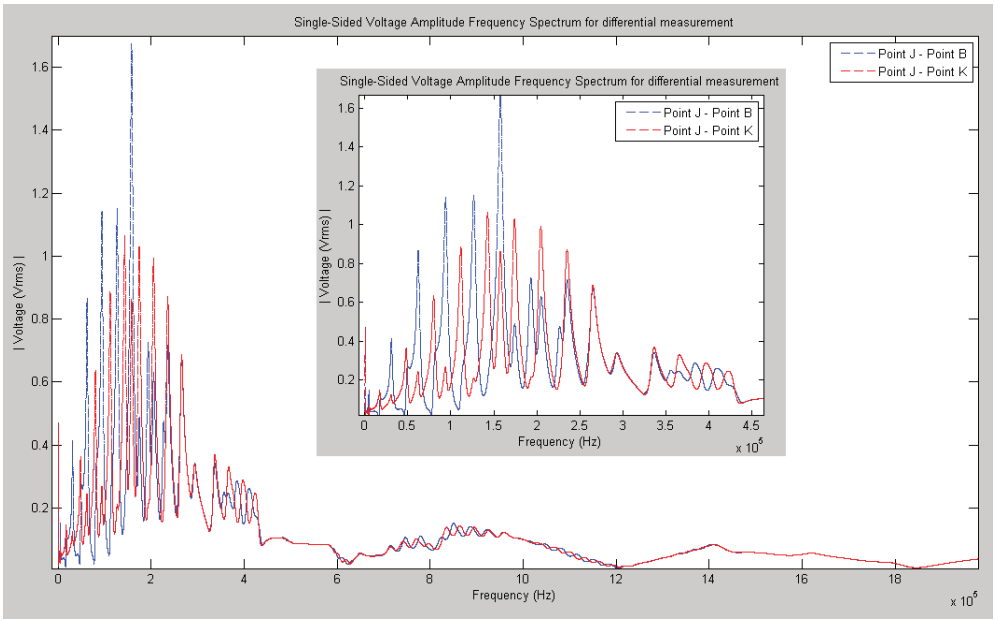

Figure C.7 Single-Sided Voltage Amplitude Frequency spectrum for Differential Measurement with the measurement on either side of thumper (Point B and Point K) not shifted in time to represent synchronous differential measurement